Identification of chemotaxis compounds in root exudates and their sensing chemoreceptors in plant growth-promoting rhizobacteria *Bacillus amyloliquefaciens* SQR9

Running title: Root-secreted chemoattractant and receptor of PGPR

Haichao Feng[1,2], Nan Zhang[1], Wenbin Du[3], Huihui Zhang[1], Yunpeng Liu[2], Ruixin Fu[1], Jiahui Shao[1], Guishan Zhang[2], Qirong Shen[1], Ruifu Zhang[1,2*]

[1]Jiangsu Provincial Key Lab for Organic Solid Waste Utilization, National Engineering Research Center for Organic-based Fertilizers, Jiangsu Collaborative Innovation Center for Solid Organic Waste Resource Utilization, Nanjing Agricultural University, Nanjing, 210095, P.R. China

[2]Key Laboratory of Microbial Resources Collection and Preservation, Ministry of Agriculture, Institute of Agricultural Resources and Regional Planning, Chinese Academy of Agricultural Sciences, Beijing 100081, P.R. China

[3]State Key Laboratory of Microbial Resources, Institute of Microbiology, Chinese Academy of Sciences, Beijing 100101, China

[*]**Corresponding author** Ruifu Zhang, College of Resources and Environmental Sciences, Nanjing Agricultural University, Nanjing, 210095, P.R. China. E-mail: rfzhang@njau.edu.cn, Tel: 86-025-84396477, Fax: 86-025-84396260

ABSTRACT: Chemotaxis-mediated response to root exudates, initiated by sensing-specific ligands through methyl-accepting chemotaxis proteins (MCPs), is very important for root colonization and beneficial functions of plant growth-promoting rhizobacteria (PGPRs). Systematic identification of chemoattractants in complex root exudates and their sensing chemoreceptors in PGPRs is helpful for enhancing their recruitment and colonization. In this study, 39 chemoattractants and 5 chemorepellents, including amino acids, organic acids and sugars, were identified from 98 tested components of root exudates for the well-studied PGPR strain *Bacillus amyloliquefaciens* SQR9. Interestingly, mutant stain SQR9Δ*8mcp* with all eight putative chemoreceptors completely deleted lost the chemotactic responses to those 44 compounds. Gene complementation, chemotaxis assay and isothermal titration calorimetry analysis revealed that McpA was mainly responsible for sensing organic acids and amino acids, while McpC was mostly for amino acids. These two chemoreceptors may play important roles in the rhizosphere chemotaxis of SQR9. In contrast, the *B. amyloliquefaciens*-unique chemoreceptor McpR was specifically responsible for arginine, and residues Tyr-78, Thr-131 and Asp-162 were critical for arginine binding. This study not only deepened our insights into PGPR-root interaction but also provided useful information to enhance the rhizosphere chemotaxis mobility and colonization of PGPRs, which will promote their application in agricultural production.

KEYWORDS: Chemotaxis, Plant growth-promoting rhizobacteria, Methyl-accepting chemotaxis protein, Root exudates

INTRODUCTION

Plant growth-promoting rhizobacteria (PGPRs) are widely used in agricultural production for stimulating plant growth and suppressing soil-borne diseases (Lugtenberg and Kamilova, 2009), but the performance of their plant-beneficial effects depends on efficient rhizosphere colonization (Compant et al., 2010). Chemotaxis, the ability of motile bacteria to direct their movement in gradients of attractants and repellents, plays an important role during the rhizosphere colonization process of PGPRs. In the rhizosphere, a nutrient gradient is formed by plant-released root exudates, which have a complex composition and include some components that may serve as chemoattractants or chemorepellents for plant beneficial microbes (Badri and Vivanco, 2009; Liu et al., 2017). Root exudate-mediated chemotaxis is recognized as the initial step of the recruitment and colonization process (De et al., 2002; Zhang et al., 2014; Scharf et al., 2016), which enhances the ability of bacteria to colonize the roots of diverse plant hosts (Caetano-Anollés et al., 1988; Bais et al., 2006; Berendsen et al., 2012; Scharf et al., 2016).

Bacterial chemotaxis is triggered when a stimulating molecule binds to its cognate chemoreceptor. Typical chemoreceptors are composed of a methyl-accepting (MA) domain, a cytosolic signaling domain, a HAMP (histidine kinase, adenyl cyclase, methyl-accepting chemotaxis protein and phosphatase) linker (Aravind and Ponting, 1999), and a ligand-binding domain (LBD), which is frequently located in the extracytoplasmic space and is responsible for binding extracellular compounds (Milburn et al., 1991; Baker et al., 2006). The binding of the ligand to LBD modulates the autophosphorylation of the histidine kinase CheA, which in turn transfers the phosphoryl groups to the response regulator CheY.

Subsequently, the generated CheY-P permits its interaction with the flagellar motor (FliM) to control cell swimming or tumbling and to ultimately mediate chemotaxis (Sourjik and Wingreen, 2012).

A large number of chemoreceptors and their corresponding ligands have been characterized in different microorganisms, including *Escherichia coli*, *Pseudomonas putida*, *Bacillus subtilis* and *Sinorhizobium meliloti* (Garrity and Ordal, 1995; Sourjik, 2004; Yssel et al., 2011; Sampedro et al., 2015; Webb et al., 2017). Five chemoreceptors (Tar, Tsr, Tap, Trg, and Aer) have been identified in *E. coli*, which responds to concentration gradients of amino acids, dipeptides, and sugars (Sourjik, 2004). Twenty-seven MCPs from the free-living environmental bacterium *P. putida* KT2440 have been characterized, while McpS, McpP, and McpQ are found to be chemoreceptors for tricarboxylic acid cycle intermediates, C_2 and C_3 carboxylic acids, and citrate/metal ion complexes, respectively (Sampedro et al., 2015). The Gram-positive model bacterium *B. subtilis* possesses 10 MCPs, including McpA, McpB, McpC, TlpA, TlpB, TlpC, HemAT, YfmS, YvaQ, and YoaH (Mowbray and Sandgren, 1998; Sourjik, 2004). McpB is found to be the sole chemoreceptor for asparagine, and McpC can directly bind 11 amino acids (proline, threonine, glycine, serine, valine, alanine, tyrosine, isoleucine, phenylalanine, leucine, and histidine) and indirectly sense four others (lysine, arginine, methionine, and glutamine). The myoglobin-like transducer HemAT is responsible for aerotaxis (Hou et al., 2000).

Bacterial chemotaxis towards different plant-secreted molecules mediated by specific chemoreceptors in the establishment of plant-microbe interactions has been demonstrated. The chemoreceptor McpU in the alfalfa symbiont *Sinorhizobium meliloti* governed

chemotaxis towards host plant root exudates following colonization through direct proline sensing (Webb et al., 2014). Similarly, the chemotaxis receptor IcpB sensing oxygen in *Azorhizobium caulinodans* modulated nodulation and nitrogen fixation on the stems and roots of *Sesbania rostrata* (Jiang et al., 2016). The CtaA, CtaB, and CtaC receptors in *Pseudomonas fluorescens* Pf0-1 are responsible for sensing amino acids in root exudates and play an important role in root colonization (Oku et al., 2012). Recently, multiple chemotaxis receptors (including McpB, McpC, and TlpC) were found to be involved in the intact chemotaxis of *B. subtilis* 3610 to *Arabidopsis thaliana* root exudates, and this process was required for bacterial colonization (Allard-Massicotte et al., 2016).

However, the chemical composition of root exudates is extremely complex, and the chemotaxis behavior of PGPR to root exudates is integrative effects of all root-secreted chemoattractants and chemorepellents. Systematic identification of chemoattractants and chemorepellents in root exudates and elucidation of how these various root-secreted compounds are sensed by multiple chemoreceptors of a PGPR strain could give us a comprehensive understanding of PGPR chemotaxis in the rhizosphere. In this study, *B. amyloliquefaciens* SQR9, a well-studied and commercially widely used PGPR strain, which showed chemotaxis toward root exudates and formed obvious biofilms on plant roots(Weng et al., 2013; Liu et al., 2017), was used to explore the chemotaxis compounds in root exudates. The objectives of this study were (i) to detect the chemoattractants (or chemorepellents) in root exudates sensed by SQR9 and (ii) to identify the SQR9 chemoreceptors involved responsible for these detected compounds. These results will provide guidelines to enhance the rhizosphere colonization and beneficial function of PGPRs in agricultural production.

RESULTS

Identification of chemotactic compounds for PGPR strain *B. amyloliquefaciens* SQR9 in root exudates

B. amyloliquefaciens SQR9 (**Table 1**) was isolated from the cucumber rhizosphere and showed positive chemotactic responses to root exudates (Weng et al., 2013; Liu et al., 2017). Also, the transcription of its chemotaxis and motility genes was up-regulated by root exudates (Zhang et al., 2015). In this study, to have a comprehensive understanding of the chemoattractants in root exudates, 98 commercially available chemical compounds were selected based on results of high-throughput analysis of cucumber root exudates conducted by Liu et al. (2017); this analysis included sugars, sugar alcohols, sugar acids, amines, amino acids, fatty acids, organic acids and others (**Table 2**). These chemicals were tested individually for the chemotactic response of SQR9 using a simple and reusable microfluidic SlipChip device as described by Shen et al. (2014). Results showed that SQR9 has a chemotactic response to 44 of these 98 tested compounds (**Table 2 & Table S1**). Among them, 23 compounds were strong chemoattractants with a chemotaxis index (I_{30}) of more than 0.8 (**Table 2**). Sixteen compounds were demonstrated as medium chemoattractants with an I_{30} between 0.6 and 0.8 (**Table 2**). Additionally, few root exudate compounds (DL-dithiothreitol, hydroxycarbamate, pentadecanoic acid, salicylic acid and sodium decanoate) were characterized as repellents for SQR9 with an I_{30} less than 0.4. These results indicated that most of these responsive components served as chemoattractants, which may explain the general positive chemotactic response of SQR9 to total root exudates as reported previously (Weng et al., 2013; Liu et al., 2017). However, more than half (54 of 98) of the tested

components did not have any chemotaxis effect on SQR9 (**Table S1**).

Detection of MCPs in *B. amyloliquefaciens* SQR9

Chemoattractants or chemorepellents are sensed by bacterial chemoreceptors. To elucidate how these identified root secreted compounds were recognized by SQR9, the potential MCPs genes were predicted according to the existing of methyl-accepting (MA) domain (Alexander and Zhulin, 2007) by using the whole genome sequence of SQR9 (NCBI accession no. CP006890) (Zhang et al., 2015). Eight potential MCP encoding genes were detected, which included *mcpA* (V529_30840), *mcpB* (V529_30860), *mcpC* (V529_13280), *tlpA* (V529_30850), *tlpB* (V529_30830), V529_10510, *hemAT* (V529_09980), and *yfmS* (V529_06960) (**Figure 1A**). Compared with the well-studied *B. subtilis* strains 168 and OI1085, seven predicated MCPs in SQR9 were conserved, and a unique chemoreceptor gene V529_10510 (designated as *mcpR*) was found to only exist in SQR9 (**Figure 1B**). *B. amyloliquefaciens* SQR9 appeared to have fewer MCPs, since three chemoreceptors (TlpC, YoaH, and YvaQ) of strain 168 were found to be absent in SQR9. According to the report of Yssel et al. (2011), the similarity of homologous chemotaxis proteins between *B. subtilis* and *B. amyloliquefaciens* was only about 70%. These findings suggested that though being close-related organisms, the specific functions of MCPs in *B. amyloliquefaciens* are quite different from those in *B. subtilis*.

The domain architecture analysis of the eight predicated MCPs based on the SMART database (Schultz et al., 1998) indicated that, except for HemAT and YfmS, the predicted extracellular domain was existed in all other six MCPs, and five of them (excluding McpR) had a conserved ligand binding domain (LBD) for sensing environmental signals (**Figure 1A**).

The LBDs of McpA, McpB, McpC, TlpA and TlpB in *B. amyloliquefaciens* SQR9 contain dCache domains and belong to cluster II based on their molecular sizes (239, 246, 242, 239, and 245 amino acids, respectively). However, the LBD of McpR contains CHASE3 and belongs to cluster I (138 amino acids).

BLAST analysis based on the McpR amino acid sequence retrieved 67 alignments that shared high similarity (identity>51%; including McpR itself) in NCBI (**Table S2**), most of which originated from *B. amyloliquefaciens* and *B. velezensis* (30 alignments for each). Additionally, sequences from *B. nakamurai* (2 alignments), *B. subtilis* (1 alignment), and *Bacillus sp.* (3 alignments) were also obtained. *B. amyloliquefaciens* and *B. velezensis* are considered to be a taxonomic unit above the species level and form "operational group *B. amyloliquefaciens*" within the *B. subtilis* species complex (Fan et al., 2017). More than 50% of *B. amyloliquefaciens* (55.4%) and *B. velezensis* (53.6%) strains contain McpR, while only 12.5 % *B. nakamurai* strains and 1.8 % *B. subtilis* strains contain McpR. These analyses indicate that McpR may be a unique chemoreceptor of *B. amyloliquefaciens*.

SQR9Δ*8mcp* deficient in all eight putative *mcp* genes completely lost chemotactic reaction to 44 compounds

To elucidate the roles of these detected MCPs in SQR9's chemotactic response to these root-secreted chemoattractants and chemorepellents, all eight MCP-encoding genes were deleted from the SQR9 genome to obtain the strain SQR9Δ*8mcp*. Chemotaxis experiments of SQR9Δ*8mcp* with the 44 identified chemoattractants and chemorepellents showed that SQR9Δ*8mcp* completely lost the chemotaxis ability to the 44 compounds (**Table 2**). These results suggest that these eight predicted genes encode the major functional MCPs, which are

172 critical for SQR9's chemotactic response to root-secreted chemoattractants and
173 chemorepellents.

174 **McpA is a major chemoreceptor of SQR9 for a broad range of chemoattractants**

175 To determine the chemoreceptor responsible for these root-secreted chemoattractants and
176 chemorepellents, each of the eight MCP encoding genes was individually complemented in
177 SQR9Δ*8mcp,* and the chemotaxis of the complementary strains to these 44 compounds were
178 tested. Expression of McpA (SQR9Δ*8mcp*/*mcpA*) significantly restored chemotaxis to 20
179 compounds (**Figure 2A**), including five amino acids (aspartic acid, glutamic acid, isoleucine,
180 lysine, and tyrosine), ten organic acids (citric acid, malic acid, oxalic acid, fumaric acid,
181 succinic acid, phthalic acid, adipic acid, dehydroascorbic acid, glyceric acid, and
182 3-hydroxypropionic acid), and five other compounds (hydroxycarbamate, mannose, ribose,
183 fucose, and ribitol). SQR9Δ*8mcp*/*mcpA* also partially restored the chemotactic reaction to
184 sodium decanoate, serine, gluconic acid, and fructose, indicating that McpA probably
185 participated in, but did not dominate, the chemotaxis to these compounds (**Table 3 & Table**
186 **S3**). These results suggest that McpA senses a broad range of root-secreted compounds and is
187 a major chemoreceptor of SQR9.

188 To further verify the above chemotaxis assay, the amino-terminal sensing domain of
189 McpA (Ala33- Pro278) was expressed and purified (**Figure S1A**), and its binding of citric
190 acid and aspartic acid (represent the McpA sensed organic acids and amino acids, respectively)
191 was investigated using isothermal titration calorimetry (ITC) analysis. The ITC results
192 indicated that the LBD of McpA directly bound the two compounds *in vitro* and that the
193 binding reactions were exothermic, with a K_D value of 0.39±0.15 and 0.24±0.16 μM for citric

194 acid and aspartic acid, respectively. The Δ*H* values for the two ligands were calculated to be
195 -14.34±0.47 kcal mol^{-1} and -10.37±0.48 kcal mol^{-1}, respectively (**Figure 2B**).

196 **Other chemoreceptors of SQR9 were responsible for fewer compounds**

197 Compared with McpA, other chemoreceptors of SQR9 showed a relatively narrow
198 binding ligand range (**Figure 3A**). Complementation of *hemAT* and *yfmS*
199 (SQR9Δ*8mcp*/*hemAT* and SQR9Δ*8mcp*/*yfmS*) did not have any chemotactic effect regarding
200 to these tested compounds (**Table S4**). Thus, these two genes were not involved in the
201 chemotaxis of SQR9 to the root-secreted compounds, which may be due to their lack of
202 extracellular region. For the 44 tested compounds, McpB was only responsible for four amino
203 acid attractants (glycine, tryptophan, asparagine, and glutamine), as well as two
204 chemorepellents, salicylic acid and sodium decanoate (**Figure 3A**). McpC was mostly
205 responsible for amino acids, since nine of the SQR9Δ*8mcp*/*mcpC* restored chemoattractants
206 were amino acids (valine, alanine, threonine, proline, serine, leucine, cystine, methionine, and
207 histidine) (**Figure 3A**). TlpA only showed a response to a chemorepellent, DL-dithiothreitol,
208 while TlpB responded to five chemoattractants (phenylalanine, maltose, fructose, dulcitol and
209 inosine), mostly sugars, and a potential chemorepellent of pentadecanoic acid verified by ITC
210 subsequently (**Figure 3A**).

211 ITC analysis of the purified LBDs of McpB (Glu33- Pro278), McpC (Lys33- Met274),
212 TlpA (Ala33- Pro278) and TlpB (Ala33- Met282) **(Figure S1B & 1C & 1D)** with certain
213 compounds was conducted to verify the results of the chemotaxis experiments of
214 complementary strains (**Figure 3B**). The K_D and Δ*H* values for McpBLBD and sodium
215 decanoate binding were 3.44±2.17 μM and -1.30±0.18 kcal mol^{-1}, respectively, the K_D values

for binding of McpCLBD with leucine and proline were 3.64±0.78 and 3.62±0.78 μM, respectively, and the Δ*H* values were calculated to be -81.05±7.01 and -85.63±7.48 kcal mol^{-1}, respectively. The K_D and Δ*H* values for the binding of TlpBLBD with phenylalanine and pentadecanoic acid were 3.17±0.89 and 3.03±0.66 μM, -32.24±3.39 and -25.68±1.86 kcal mol^{-1}, respectively.

The unique chemoreceptor McpR in *B. amyloliquefaciens* specifically mediates chemotaxis to arginine

McpR is a unique chemoreceptor of *B. amyloliquefaciens*. Complementation of McpR (SQR9Δ*8mcp*/*mcpR*) fully restored the chemotactic response to arginine, but not to the other 19 amino acids (**Table S5**). Furthermore, the sensing of arginine by McpR was specific in SQR9. The other seven chemoreceptor gene complementary strains did not show chemotactic response to arginine (**Figure 4A**), and SQR9Δ*8mcp*/*mcpR* hardly showed any chemotactic response to the other tested compounds, except a slight positive chemotaxis towards succinic acid and fucose with very low I_{30} values compared with the other seven chemoreceptor gene complementary strains, which suggested that McpR may partially participate in the response to succinic acid and fucose (Data not shown). The expressed and purified amino-terminal sensing domain of McpR (Ser35- Gln165) (**Figure S1E**) directly bound to arginine *in vitro* in the ITC analysis with K_D and Δ*H* values of 8.38±1.41 μM and 40.36±1.91 kcal mol^{-1}, respectively (**Figure 4B**).

To further uncover the potential arginine binding residues in the McpR-LBD, the sequences of the reported chemoreceptors for arginine were obtained. The McpC in *B. subtilis* OI1085 was reported to bind L-Arg with significantly higher affinity (K_D of approximately

100 μM) (Glekas et al., 2012), while McpB was also involved in chemotaxis to L-Arg (Yssel et al., 2011). Both PctA-LBD and PctB-LBD of *Pseudomonas aeruginosa* PAO1 could bind L-Arg with a K_D of 1 μM and 60 μM, respectively and PctA is the major receptor for L-Arg (Rico-Jimenez et al., 2013). Amino acid sequence alignment (using ClustalW and MAFFT) of the five arginine receptor LBDs revealed that residues Tyr-78, Asp-162 and Thr-131 may be crucial for arginine binding in McpR of SQR9 (**Figure S2**). For confirmation, these three residues were individually substituted by glycine, which cannot form hydrogen bonds with small ligands and is the smallest amino acid, to avoid causing possible structure disruption in the putative binding pockets. Chemotaxis analysis demonstrates that the three SQR9Δ*8mcp*/*mcpR* strains with single amino acid mutations of *mcpR* showed significantly decreased chemotaxis to arginine compared with wild-type *mcpR* (**Figure 5**). Taken together, these results showed that the residues Tyr-78, Thr-131 and Asp-162 are the amino acid residues in McpR that are involved in arginine binding.

DISCUSSION

B. amyloliquefaciens SQR9 is a plant beneficial rhizobacterium with a strong root colonization capability and positive chemotaxis towards cucumber root exudates (Weng et al., 2013), whose composition has been identified through GC-MS (Liu et al., 2017). In this study, we show that PGPR strain *B. amyloliquefaciens* SQR9 chemotactically responded to nearly half of the tested root exudate components (44 of the 98 compounds); 39 of them were chemoattractants, while only 5 compounds served as chemorepellents. Amino acids, organic acids and sugars, were the major chemoattractant compounds, which accounted for 45%, 32% and 11% of the identified chemoattractants, respectively. The chemoreceptors McpA and

McpC, which are mainly responsible for sensing amino acids and organic acid chemoattractants, may play critical roles in the chemotaxis mobility of SQR9 to the plant root (**Figure 6**).

Generally, root exudates were divided into two different classes of compounds: the low-molecular-weight compounds, including a variety of amino acids, organic acids, sugars, and secondary metabolites, and high-molecular-weight compounds, including proteins and polysaccharides (Badri and Vivanco, 2009; Liu et al., 2017). So far, most of the identified chemoattractants of root exudates for rhizobacteria were low-molecular-weight compounds, which are carbon and energy resources in the environment. Additionally, chemotaxis is believed to assist rhizobacteria in moving to areas suitable for growth (Szurmant and Ordal, 2004; Lacal et al., 2010; Porter et al., 2011; Jiang et al., 2016).

As an important microorganism that is closely related to *B. amyloliquefaciens*, *B. subtilis* OI1085 showed a chemotaxis response to all 20 L-amino acids, which were predominantly mediated by McpC (supports chemotaxis to 17 and directly binds to 11 amino acids) and McpB (supports chemotaxis to four amino acids) (Hanlon and Ordal, 1994). Here, we found that the sensing of amino acids in *B. amyloliquefaciens* SQR9 was dispersed among different chemoreceptors, which is significantly different from *B. subtilis* OI1085. In SQR9, McpA, McpB, McpC, TlpB, and McpR responded to 6, 7, 9, 2 and 1 amino acid(s), respectively (**Table 3 & Table S3**). Interestingly, the extracellular regions of the chemoreceptors McpA, McpB, and McpC of SQR9 were similar to the chemoreceptors McpB and McpC of *B. subtilis*, which were predicted to possess double PDC sensor domains (Glekas et al., 2010; Glekas et al., 2012; Rico-Jimenez et al., 2013; Sampedro et al., 2015). McpC was the

dominant amino acid sensor in SQR9, since nine of ten of its ligands were amino acids (**Table 3 & Table S3**). Amino acid sequence alignments showed that the identities of McpC-LBD between SQR9 and OI1085 were 61.63%.

More than 140 compounds have been found to induce chemotaxis in *Pseudomonas* strains (Sampedro et al., 2015), which made these strains models for establishing chemoreceptor structure-function relationships (Kato et al., 2008). Garcia et al. (2015) reported that McpP of *Pseudomonas putida* KT2440 had a CACHE-type LBD and mediated taxis to some C_2 and C_3 carboxylic acids. In this study, the large-scale identification of chemoattractants in root exudates and their responsible chemoreceptors in SQR9 facilitated the revealing of the chemoreceptor structure-function relationship. Among the 20 ligands of McpA, nine compounds had carboxyl groups at both ends of the chains, which included two amino acids (aspartic acid and glutamic acid) and seven acids (citric acid, malic acid, oxalic acid, fumaric acid, succinic acid, phthalic acid, and adipic acid) (**Figure S3**). McpA had a dCache domain, which was different from the CACHE domain of McpP in *Pseudomonas putida* KT2440. In SQR9, McpC predominantly mediated the chemotaxis to aliphatic amino acids (leucine, alanine, and valine), sulfur-bearing amino acids (cystine and methionine), and hydroxy amino acids (threonine and serine), and McpB seemed to mediate the chemotaxis to the only two amide amino acids, asparagine and glutamine. These results suggest that compounds with similar structure may be sensed by the same chemoreceptor.

Compounds that are attractants for some bacteria may be repellents for others. For example, acetate is an attractant for *R. sphaeroides* but a repellent for *E. coli* (Tso and Adler, 1974; Packer and Armitage, 2000). Interestingly, a compound can switch from being an

attractant at a low oxygen concentration to a repellent at atmospheric oxygen concentrations, depending on the growth conditions and the needs of the *R. sphaeroides* cell (Romagnoli et al., 2002). In our work, though 1 mM concentration of the tested ligands in the chemotaxis assay was higher than their actual concentration in the rhizosphere, the SlipChip device allowed the formation of diffusion concentration gradients of the chemoeffector, which mimics the natural condition that plant-released root exudates form a nutrient gradient with distance (Shen et al., 2014). Under this condition, a substantial amount of the tested root exudate components were sensed by SQR9 as chemoattractants, while only a few compounds were chemorepellents. These results reinforce the ideas that many PGPR strains show strong chemotactic responses to root exudates, which are very important for the beneficial functions of PGPRs.

ITC analysis *in vitro* is an important approach for verifying whether the binding between chemoreceptor and ligand is direct or not. In this study, the dominant objectives were focused on identification of the MCPs mediating chemotactic response of SQR9 to the 39 chemoattractants and 5 chemorepellents by direct binding or other ways. To explore the correspondence between these ligands and their potential MCPs, we randomly picked eight representative compounds to perform the ITC analysis, and excitedly found that all of them can directly bind to the identified chemoreceptors in SQR9.

In conclusion, we have identified 44 compounds in root exudates that the plant-beneficial rhizobacterium *B. amyloliquefaciens* SQR9 chemotactically responded to, 39 of which served as attractants to recruit SQR9 to colonize in the rhizosphere. Among the multiple chemoreceptors of the PGPR strains, the receptors mainly responsible for the root-secreted organic acids and amino acids may play important roles in the rhizosphere chemotaxis

mobility of PGPRs. These results not only deepened our insights of PGPR-root interaction but also provided useful information to enhance the rhizosphere chemotaxis mobility and colonization of PGPRs with the *in vitro* addition of a suitable chemoattractant. This approach will increase the efficiency of PGPRs in agricultural production and reduce the input of chemical fertilizers and pesticides.

MATERIALS AND METHODS

Bacterial strains, media and growth conditions

The strains and plasmids used in this study are described in **Table 1**. *B. amyloliquefaciens* SQR9 (China General Microbiology Culture Collection Center, CGMCC accession no. 5808) was isolated from the cucumber rhizosphere. SQR9 was grown at 37°C in low-salt Luria-Bertani (LLB) medium (peptone, 10 g L^{-1}; yeast extract, 5 g L^{-1}; NaCl, 3 g L^{-1}) that was solidified with 15 g L^{-1} agar. *Escherichia coli* BL21 (DE3) cells were grown at 37°C in Luria-Bertani (LB) medium (peptone, 10 g L^{-1}; yeast extract, 5 g L^{-1}; NaCl, 5 g L^{-1}) solidified with 15 g L^{-1} agar. When necessary, the final concentrations of antibiotics were added as follows: 5 mg L^{-1} chloramphenicol (Cm); 20 mg L^{-1} zeocin (Zeo); 100 mg L^{-1} spectinomycin (Spc); 30 mg·L^{-1} kanamycin (Kan).

Methyl-accepting chemotaxis protein (MCP) gene prediction and deletion in *B. amyloliquefaciens* SQR9

Based on the whole genome sequence of *B. amyloliquefaciens* SQR9 (NCBI accession no. CP006890) (Zhang et al., 2015), the potential genes encoding for MCPs were predicated according to the standard existence of a methyl-accepting (MA) domain (Alexander and Zhulin, 2007).

Considering the functional redundancy of MCPs for sensing chemoeffectors as reported in many organisms (Glekas et al 2012, Ni et al 2013, Oku et al 2012, Webb et al 2014), the *B. amyloliquefaciens* SQR9 mutant deficient in all eight predicated *mcp* genes was constructed using an unmarked genetic manipulation based on multiple gene deletions that rely on a counter-selectable marker, *pheS* (Zhou et al., 2017). First, four adjacent genes (*tlpB-mcpA-tlpA-mcpB*, 8393 bp) were deleted in the first-round knockout to generate SQR9Δ*4mcp*. Then, *mcpC* (1964 bp), *mcpR* (V529_10510; 1647 bp), *hemAT* (1290 bp), and *yfmS* (852 bp) were further deleted one by one in the next rounds of knockout to finally acquire SQR9Δ*8mcp* (through SQR9Δ*5mcp*, SQR9Δ*6mcp*, and SQR9Δ*7mcp*, respectively). All these mutants were confirmed by PCR and sequencing with the primer sets listed in **Table S6**.

Complementation of the disrupted genes

The eight *mcp* genes were separately integrated into the chromosomal *amyE* locus of the chemoreceptor-deficient SQR9Δ*8mcp* to obtain single-*mcp*-gene complementary strains (SQR9Δ*8mcp*/*mcpA*, SQR9Δ*8mcp*/*mcpB*, SQR9Δ*8mcp*/*mcpC*, SQR9Δ*8mcp*/*tlpA*, SQR9Δ*8mcp*/*tlpB*, SQR9Δ*8mcp*/*mcpR*, SQR9Δ*8mcp*/*hemAT* and SQR9Δ*8mcp*/*yfmS*). First, the full sequence of each of the eight *mcp* genes (*mcpA*, *mcpB*, *mcpC*, *tlpA*, *tlpB*, *mcpR*, *hemAT*, and *yfmS*) with its native promoter was amplified from SQR9 genomic DNA, with primer sets summarized in **Table S6**, which partially overlapped with chloramphenicol or spectinomycin resistance genes (Cm^R or Spc^R) and the downstream fragments. After that, an upstream 0.70-kb fragment and a downstream 0.74-kb fragment of the 1.97-kb *amyE* gene were amplified with the primer set *amyE*-UF/*amyE*-UR (**Table S6**). Subsequently, the 1.0-kb

370 *Cm*^{R} and *Spc*^{R} genes were amplified from the plasmid pNW33n and p7S6 (Yan et al., 2008)
371 with primer sets P1/P2 and P3/P4, respectively (**Table S6**), which overlapped with the
372 upstream fragments and the complemented genes. Finally, the obtained four fragments were
373 fused by overlap PCR, and the fused fragments for each of the eight target genes were
374 individually transformed into Δ*8mcp* competent cells. The obtained transformants were
375 verified using primer sets shown in **Table S6** (Zhou et al., 2017).

376 **Chemotaxis assay**

377 The chemotaxis assay was performed as described in Shen et al. (2014) by using a simple
378 and reusable microfluidic SlipChip device. By a simple slipping operation, three microwells
379 were disconnected from other units and interconnected by the ducts, which allowed the
380 formation of diffusion concentration gradients of the chemoeffector for inducing cell
381 migration from the cell microcells towards the other two microwells. As a result, the
382 concentration of the chemoeffector sensed by bacteria is lower than its initial concentration.
383 Briefly, a 10-mg mL^{-1} bovine serum albumin (BSA) solution was injected into all channels
384 and used to wash the microwells for 5 min. After removing the BSA solution using a vacuum
385 across the access holes, the solutions containing different chemoeffectors, bacterial cells
386 suspended in PBS buffer (8 g L^{-1} NaCl, 0.2 g L^{-1} KCl, 1.44 g L^{-1} Na_2HPO_4, 0.24 g L^{-1} KH_2PO_4,
387 pH 7,4), and PBS buffer (negative control) were loaded to the top, middle, and bottom
388 microwells, respectively. Subsequently, the SlipChip device was slipped to ensure that the
389 cells could migrate freely from the middle microwells to the ducts and the microwells were
390 loaded with the chemoeffector or PBS. The device was placed on an inverted fluorescence
391 microscope (Ti-Eclipse, Nikon, Japan) and kept for 30 min in the dark at room temperature.

Then, the cells in the top microwells and bottom microwells were monitored. The chemotaxis index (I_t) was used to indicate the chemotactic ability of the bacterial cells with a chemoeffector at a certain concentration. I_t was defined as $N_e/ (N_e + N_c)$, where N_e is the number of cells that migrated into the chemoeffector-containing microwells, and N_c is the number of cells that migrated into the control microwells in a certain time period.

$$I_t=N_e/ (N_e+N_c)$$

In this study, I_{30} was used to characterize chemotaxis, cells were allowed to migrate freely in the gradient for 30 min. In theory, an I_{30} value approximately equal to 0.5 means that the cells do not respond to the chemoeffector, while an I_{30} value more than 0.5 indicates that the cells are attracted by the chemoeffector and an I_{30} value lower than 0.5 suggests the cells are repelled by the chemoeffector. Here, to ensure the stability and reliability of the assessment, we redefined the non-response interval of I_{30} to the range between 0.4 and 0.6, while >0.6 and <0.4 were defined as positive and negative responses to the chemoeffector, respectively.

Protein expression and purification

Expression and purification of the ligand binding domain (LBD) of McpA, McpB, McpC, TlpA, TlpB, and McpR in *B. amyloliquefaciens* SQR9 was performed. The DNA fragments encoding the LBD of McpA (Ala33- Pro278), McpB (Glu33- Pro278), McpC (Lys33- Met274), TlpA (Ala33- Pro278), TlpB (Ala33- Met282), and McpR (Ser35- Gln165) were amplified with primer sets that contained restriction sites for *NdeI* and *HindIII* (**Table S6**) using SQR9 genomic DNA as a template. The PCR products were digested and cloned into the expression plasmid pET28a (+), which was linearized with the *NdeI* and *HindIII* enzymes.

The insert and flanking regions of the six reconstructed plasmids (being pET28a-McpALBD, pET28a-McpBLBD, pET28a-McpCLBD, pET28a-TlpALBD, pET28a-TlpBLBD, and pET28a-McpRLBD) were verified by DNA sequencing. The expressed proteins contained an N-terminal His tag.

The six constructed expression vectors were individually introduced into *Escherichia coli* BL21 (DE3). The obtained strains were grown in 1 L Erlenmeyer flasks containing 200 mL of LB medium supplemented with 30 mg L^{-1} kanamycin at 37°C with 220 rpm shaking. When the OD_{600} of the culture reached 0.6, the growth temperature was lowered to 16°C. After another 30-min incubation, the protein expressions were induced by adding 0.05 mM isopropyl-β-D-thiogalactopyranoside (IPTG). The growth was continued at 16°C with 220 rpm shaking overnight prior to cell harvest by centrifugation at 8,000 g for 10 min. Then, the cells were washed at least twice with 0.01 M PBS. The cell pellets were resuspended in 50 mL of 0.01 M PBS and disrupted by sonication (2-s pulse on, 3-s pulse off). The cellular lysates were centrifuged at 20,000 g for 50 min. Finally, for further clarification, the lysates were passed through a 0.22 μm filter (Millipore) to remove any other aggregates or insoluble particles, followed by purification with His-affinity resin chromatography according to the manufacturer's (Hua Chun, Tianjin) instructions. All the purified proteins were collected and stored in TKMDmod buffer (50 mM Tris, pH 8.0, 50 mM KCl, 5 mM $MgCl_2$) at -80°C.

Isothermal titration calorimetry

All isothermal titration calorimetry (ITC) measurements were performed using an iTC200 titration calorimeter (MicroCal, GE) at 25°C, and the data were extracted and processed using the Origin software package. All the ligands were dissolved in TKMDmod

buffer. For ligand binding analysis, the protein was placed into the sample cell and was titrated with aliquots of ligand solution in the injector syringe. The 400 μL reaction cell was constantly stirred at 750 rpm. The mean enthalpies measured from the injection of the ligands into the buffer were subtracted from raw titration data prior to data analysis using the 'One binding site model' of the MicroCal version of ORIGIN. The two important constants, the apparent dissociation constants (K_D) and the enthalpy change (ΔH), were gained. The smaller the K_D value, the stronger the binding of the protein and ligand is. Moreover, the binding is endothermic, while the ΔH is greater than zero. When the ΔH is less than zero, the binding is exothermic.

SUPPLEMENTARY DATA

Figure S1 SDS-PAGE analysis of the proteins after purification.

Figure S2 Sequence alignments of chemoreceptor sensing domains performed by ClustalW (A) and MAFFT (B).

Figure S3 Nine compounds with carboxyl groups at both ends of the chains within the 44 attractants or repellents.

Table S1. The 54 chemical compounds not chemotactically responded by *B. amyloliquefaciens* SQR9.

Table S2. The overview of *mcpR*-containing strains.

Table S3. Chemotaxis index of the 18 compounds sensed by more than one *mcp*-gene for *B. amyloliquefaciens* SQR9, chemoreceptor-deficient mutant SQR9Δ8mcp and the single-*mcp*-gene complementary strains.

Table S4. Chemotaxis index of the 44 compounds for *hemAT* and *yfmS* gene complementary

strains *B. amyloliquefaciens* SQR9Δ*8mcp/hemAT* and SQR9Δ*8mcp/yfmS*.

Table S5. The Chemotaxis index of 20 essential amino acids for *B. amyloliquefaciens* SQR9, chemoreceptor-deficient mutant SQR9Δ*8mcp* and the *mcpR* complementary strain SQR9Δ*8mcp/mcpR*.

Table S6. Primers used in this study.

ACKNOWLEDGMENTS

This work was financially supported by National Natural Science Foundation of China (31672232, 31572214, 31330069 and 31500081), the National Key Basic Research Program of China (973 program, 2015CB150505) and the National Key Research and Development Program (2016YFD0200305 and 2017YFD0200805). R. Z and Q. S were also supported by the Key Projects of International Cooperation in Science and Technology Innovation (2016YFE0101100), the 111 Project (B12009) and the Priority Academic Program Development (PAPD) of Jiangsu Higher Education Institutions. We thank Dr. Jun Luo (Nanjing University) for the help in ITC experiments, Dr. Dongwei Chen (Chinese Academy of Sciences) for the help in chemotaxis assay, and Dr. Youzhi Miao (Nanjing Agricultural University) for excellent technical assistance.

CONFLICT OF INTEREST

We declare that we do not have any commercial or associative interest that represents a conflict of interest in connection with the work submitted.

LITERATURE CITED

Adler, J. (1966) chemotaxis in bacteria. *Science* **153**: 708-716.

Alexander, R.P., and Zhulin, I.B. (2007) Evolutionary genomics reveals conserved structural determinants of signaling and adaptation in microbial chemoreceptors. *Proc Natl Acad Sci USA* **104**: 2885-2890.

Allard-Massicotte, R., Tessier, L., Lecuyer, F., Lakshmanan, V., Lucier, J.F., Garneau, D. et al. (2016) *Bacillus subtilis* early colonization of *Arabidopsis thaliana* roots involves multiple chemotaxis receptors. *MBio* **7**: e01664-16.

Aravind, L., and Ponting, C.P. (1999) The cytoplasmic helical linker domain of receptor histidine kinase and methyl-accepting proteins is common to many prokaryotic signalling proteins. *FEMS Microbiol Lett* **176**: 111-116.

Badri, D.V., and Vivanco, J.M. (2009) Regulation and function of root exudates. *Plant Cell Environ* **32**: 666-681.

Bais, H.P., Weir, T.L., Perry, L.G., Gilroy, S., and Vivanco, J.M. (2006) The role of root exudates in rhizosphere interactions with plants and other organisms. *Annu Rev Plant Biol* **57**: 233-266.

Baker, M.D., Wolanin, P.M., and Stock, J.B. (2006) Signal transduction in bacterial chemotaxis. *Bioessays* **28**: 9-22.

Berendsen, R.L., Pieterse, C.M., and Bakker, P.A. (2012) The rhizosphere microbiome and plant health. *Trends Plant Sci* **17**: 478-486.

Caetano-Anollés, G., Wall, L.G., De Micheli, A.T., Macchi, E.M., Bauer, W.D., and Favelukes, G. (1988) Role of motility and chemotaxis in efficiency of nodulation by *Rhizobium meliloti*. *Plant Physiol* **86**: 1228-1235.

Cao, Y., Zhang, Z., Ling, N., Yuan, Y., Zheng, X., Shen, B. et al. (2011) *Bacillus subtilis*

SQR9 can control *Fusarium* wilt in cucumber by colonizing plant roots. *Biol Fert Soils* **47**: 495-506.

Compant, S., Clément, C., and Sessitsch, A. (2010) Plant growth-promoting bacteria in the rhizo- and endosphere of plants: Their role, colonization, mechanisms involved and prospects for utilization. *Soil Biol Biochem* **42**: 669-678.

De, W.S., Vermeiren, H., Mulders, I.H., Kuiper, I., Hendrickx, N., Bloemberg, G.V. et al. (2002) Flagella-driven chemotaxis towards exudate components is an important trait for tomato root colonization by *Pseudomonas fluorescens*. *Mol Plant Microbe Interact* **15**: 1173-1180.

Dong, L., Chen, D.W., Liu, S.J., and Du, W. (2016) Automated chemotactic sorting and single-cell cultivation of microbes using droplet microfluidics. *Sci Rep* **6**: 24192.

Fan, B., Blom, J., Klenk, H.P., and Borriss, R. (2017) *Bacillus amyloliquefaciens*, *Bacillus velezensis*, and *Bacillus siamensis* form an "operational group *B. amyloliquefaciens*" within the *B. subtilis* species complex. *Front Microbiol* **8**: 22.

Garcia, V., Reyes-Darias, J.A., Martin-Mora, D., Morel, B., Matilla, M.A., and Krell, T. (2015) Identification of a chemoreceptor for C2 and C3 carboxylic acids. *Appl Environ Microbiol* **81**: 5449-5457.

Garrity, L.F., and Ordal, G.W. (1995) Chemotaxis in *Bacillus subtilis*: how bacteria monitor environmental signals. *Pharmacol Therapeut* **68**: 87-104.

Glekas, G.D., Foster, R.M., Cates, J.R., Estrella, J.A., Wawrzyniak, M.J., Rao, C.V. et al. (2010) A PAS domain binds asparagine in the chemotaxis receptor McpB in *Bacillus subtilis*. *J Biol Chem* **285**: 1870-1878.

524 Glekas, G.D., Mulhern, B.J., Kroc, A., Duelfer, K.A., Lei, V., Rao, C.V. et al. (2012) The
525 *Bacillus subtilis* chemoreceptor McpC senses multiple ligands using two discrete
526 mechanisms. *J Biol Chem* **287**: 39412-39418.

527 Hanlon, D.W., and Ordal, G.W. (1994) Cloning and characterization of genes encoding
528 methyl-accepting chemotaxis proteins in *Bacillus subtilis*. *J Biol Chem* **269**:
529 14038-14046.

530 Hida, A., Oku, S., Kawasaki, T., Nakashimada, Y., Tajima, T., and Kato, J. (2015)
531 Identification of the *mcpA* and *mcpM* genes encoding methyl-accepting chemotaxis
532 proteins (MCPs) for amino acids and L-malate and involvement of McpM-mediated
533 chemotaxis in plant infection by *Ralstonia pseudosolanacearum* (*Ralstonia*
534 *solanacearum*). *Appl Environ Microbiol* **81**: 7420-7430.

535 Hou, S., Larsen, R.W., Boudko, D., Riley, C.W., Karatan, E., Zimmer, M. et al. (2000)
536 Myoglobin-like aerotaxis transducers in Archaea and Bacteria. *Nature* **403**: 540-544.

537 Jiang, N., Liu, W., Li, Y., Wu, H., Zhang, Z., Alexandre, G. et al. (2016) A chemotaxis
538 receptor modulates nodulation during the *Azorhizobium caulinodans-Sesbania rostrata*
539 symbiosis. *Appl Environ Microbiol* **82**: 3174-3184.

540 Kato, J., Kim, H.E., Takiguchi, N., Kuroda, A., and Ohtake, H. (2008) *Pseudomonas*
541 *aeruginosa* as a model microorganism for investigation of chemotactic behaviors in
542 ecosystem. *J Biosci Bioeng* **106**: 1–7.

543 Lacal, J., Garcia-Fontana, C., Munoz-Martinez, F., Ramos, J.L., and Krell, T. (2010) Sensing
544 of environmental signals: classification of chemoreceptors according to the size of their
545 ligand binding regions. *Environ Microbiol* **12**: 2873-2884.

546 Liu, Y., Chen, L., Wu, G., Feng, H., Zhang, G., Shen, Q. et al. (2017) Identification of
547 root-secreted compounds involved in the communication between cucumber, the
548 beneficial *Bacillus amyloliquefaciens*, and the soil-borne pathogen *Fusarium oxysporum*.
549 *Mol Plant Microbe Interact* **30**: 53-62.
550 Lugtenberg, B., and Kamilova, F. (2009) Plant-growth-promoting rhizobacteria. *Annu Rev*
551 *Microbiol* **63**: 541-556.
552 Milburn, M.V., Privé, G.G., Milligan, D.L., Scott, W.G., Yeh, J., Jancarik, J. et al. (1991)
553 Three-dimensional structures of the ligand-binding domain of the bacterial aspartate
554 receptor with and without a ligand. *Science* **254**: 1342-1347.
555 Mowbray, S.L., and Sandgren, M.O. (1998) Chemotaxis receptors: a progress report on
556 structure and function. *J Struct Biol* **124**: 257-275.
557 Ni B, Huang Z, Fan Z, Jiang CY, Liu SJ (2013). Comamonas testosteroni uses a
558 chemoreceptor for tricarboxylic acid cycle intermediates to trigger chemotactic
559 responses towards aromatic compounds. *Mol Microbiol* **90**: 813-823.
560 Oku, S., Komatsu, A., Tajima, T., Nakashimada, Y., and Kato, J. (2012) Identification of
561 chemotaxis sensory proteins for amino acids in *Pseudomonas fluorescens* Pf0-1 and their
562 involvement in chemotaxis to tomato root exudate and root colonization. *Microbes*
563 *Environ* **27**: 462-469.
564 Ordal, G.W., and Goldman, D.J. (1975) Chemotaxis away from Uncouplers of Oxidative
565 Phosphorylation in *Bacillus subtilis*. *Science* **189**: 802-805.
566 Packer, H.L., and Armitage, J.P. (2000) Behavioral responses of *Rhodobacter sphaeroides* to
567 linear gradients of the nutrients succinate and acetate. *Appl Environ Microbiol* **66**:

5186-5191.

Porter, S.L., Wadhams, G.H., and Armitage, J.P. (2011) Signal processing in complex chemotaxis pathways. *Nat Rev Microbiol* **9**: 153-165.

Rico-Jimenez, M., Munoz-Martinez, F., Garcia-Fontana, C., Fernandez, M., Morel, B., Ortega, A. et al. (2013) Paralogous chemoreceptors mediate chemotaxis towards protein amino acids and the non-protein amino acid gamma-aminobutyrate (GABA). *Mol Microbiol* **88**: 1230-1243.

Romagnoli, S., Packer, H.L., and Armitage, J.P. (2002) Tactic responses to oxygen in the phototrophic bacterium *Rhodobacter sphaeroides* WS8N. *J Bacteriol* **184**: 5590-5598.

Sampedro, I., Parales, R.E., Krell, T., and Hill, J.E. (2015) *Pseudomonas* chemotaxis. *FEMS Microbiol Rev* **39**: 17-46.

Scharf, B.E., Hynes, M.F., and Alexandre, G.M. (2016) Chemotaxis signaling systems in model beneficial plant-bacteria associations. *Plant Mol Biol* **90**: 549-559.

Schultz, J., Milpetz, F., Bork, P., and Ponting, C.P. (1998) SMART, a simple modular architecture research tool: Identification of signaling domains. *Proc Natl Acad Sci USA* **95**: 5857-5864.

Shen, C., Xu, P., Huang, Z., Cai, D., Liu, S.J., and Du, W. (2014) Bacterial chemotaxis on slipChip. *Lab Chip* **14**: 3074-3080.

Sourjik, V. (2004) Receptor clustering and signal processing in *E. coli* chemotaxis. *Trends Microbiol* **12**: 569-576.

Sourjik, V., and Wingreen, N.S. (2012) Responding to chemical gradients: bacterial chemotaxis. *Curr Opin Cell Biol* **24**: 262-268.

590 Szurmant, H., and Ordal, G.W. (2004) Diversity in chemotaxis mechanisms among the
591 bacteria and archaea. *Microbiol Mol Biol Rev* **68**: 301-319.
592 Tso, W.W., and Adler, J. (1974) Negative chemotaxis in *Escherichia coli*. *J Bacteriol* **118**:
593 560-576.
594 Webb, B.A., Helm, R.F., and Scharf, B.E. (2016) Contribution of individual chemoreceptors
595 to *Sinorhizobium meliloti* chemotaxis towards amino acids of host and nonhost seed
596 exudates. *Mol Plant Microbe Interact* **29**: 231-239.
597 Webb, B.A., Hildreth, S., Helm, R.F., and Scharf, B.E. (2014) *Sinorhizobium meliloti*
598 chemoreceptor McpU mediates chemotaxis toward host plant exudates through direct
599 proline sensing. *Appl Environ Microbiol* **80**: 3404-3415.
600 Webb, B.A., Karl Compton, K., Castaneda Saldana, R., Arapov, T.D., Keith Ray, W., Helm,
601 R.F. et al. (2017) *Sinorhizobium meliloti* chemotaxis to quaternary ammonium
602 compounds is mediated by the chemoreceptor McpX. *Mol Microbiol* **103**: 333-346.
603 Weng, J., Wang, Y., Li, J., Shen, Q., and Zhang, R. (2013) Enhanced root colonization and
604 biocontrol activity of *Bacillus amyloliquefaciens* SQR9 by *abrB* gene disruption. *Appl*
605 *Microbiol Biotechnol* **97**: 8823-8830.
606 Yan, X., Yu, H.J., Hong, Q., and Li, S.P. (2008) *Cre/lox* system and PCR-based genome
607 engineering in *Bacillus subtilis*. *Appl Environ Microbiol* **74**: 5556-5562.
608 Yssel, A., Reva, O., and Tastan Bishop, O. (2011) Comparative structural bioinformatics
609 analysis of *Bacillus amyloliquefaciens* chemotaxis proteins within *Bacillus subtilis* group.
610 *Appl Microbiol Biotechnol* **92**: 997-1008.
611 Zhang, N., Wang, D., Liu, Y., Li, S., Shen, Q., and Zhang, R. (2014) Effects of different plant

root exudates and their organic acid components on chemotaxis, biofilm formation and colonization by beneficial rhizosphere-associated bacterial strains. *Plant Soil* **374**: 689-700.

Zhang, N., Yang, D., Wang, D., Miao, Y., Shao, J., Zhou, X. et al. (2015) Whole transcriptomic analysis of the plant-beneficial rhizobacterium *Bacillus amyloliquefaciens* SQR9 during enhanced biofilm formation regulated by maize root exudates. *BMC Genomics* **16**: 685.

Zhou, C., Shi, L., Ye, B., Feng, H., Zhang, J., Zhang, R. et al. (2017) *PheS**, an effective host-genotype-independent counter-selectable marker for marker-free chromosome deletion in *Bacillus amyloliquefaciens*. *Appl Microbiol Biotechnol* **101**: 217-227.

623 **FIGURE CAPTION**

624 **Figure 1** The eight potential methyl-accepting chemotaxis proteins (MCPs) in SQR9. (A) The
625 domain architectures of the eight MCPs in the SQR9 were analyzed according to the SMART
626 database (Schultz et al., 1998). (B) Comparison of the MCPs in *B. amyloliquefaciens* SQR9
627 and *B. subtilis* 168. There were eight MCP genes in the *B. amyloliquefaciens* SQR9 genome,
628 and ten MCPs genes in *B. subtilis* 168. The double-slash stands for a substantial distance
629 between the adjacent genes.

630 **Figure 2** Chemotaxis activity mediated by the McpA chemoreceptor. (A) The chemotactic
631 responses of SQR9, SQR9Δ*8mcp* and SQR9Δ*8mcp*/*mcpA* to 20 compounds. The black dotted
632 line represents a chemotaxis index of 0.5. The concentration of all the compounds was 1 mM.
633 Data for each strain are the means of thirteen biological replicates. Error bars represent the
634 standard error of these thirteen biological replicates. Different letters above the bars indicate
635 significant differences between the three strains for each compound ($P \leq 0.05$). (B) Titration
636 of 18 μM McpALBD with 200 μM citric acid, aspartic acid, and arginine (as a negative
637 control). Upper panels contain the titration raw data and the lower panels show the integrated
638 and dilution-corrected peak areas of the raw data. Data were fitted with the 'one binding site
639 model' of the MicroCal version of ORIGIN (Amherst, MA). Abbreviations: Mali (malic acid),
640 Citr (citric acid), Oxal (oxalic acid), Succ (Succinic acid), Fuma (Fumaric acid), Phth
641 (phthalic acid), Adip (adipic acid), Asp (aspartic acid), Glu (glutamic acid), Ile (isoleucine),
642 Lys (lysine), Tyr (tyrosine), Hyca (hydroxycarbamate), Mano (mannose), Ribo (ribose), Fuco
643 (fucose), Ribi (ribitol), DeAs (dehydroascorbic acid), Glyc (glyceric acid), and 3HP
644 (3-hydroxypropionic acid).

Figure 3 Chemotaxis activity mediated by the McpB, McpC, TlpA and TlpB chemoreceptors. (A) The chemotactic responses of SQR9, SQR9Δ*8mcp*, SQR9Δ*8mcp*/*mcpB*, SQR9Δ*8mcp*/*mcpC*, SQR9Δ*8mcp*/*tlpA*, and SQR9Δ*8mcp*/*tlpB* to 23 compounds. The black dotted line represents a chemotaxis index of 0.5. The concentration of all the compounds was 1 mM. Data for each strain are the means of thirteen biological replicates. Error bars represent the standard error of thirteen biological replicates. Different letters above the bars indicate significant differences between the three strains for each compound ($P \leq 0.05$). (B) Titration of 20 μM McpBLBD, 20.5 μM McpCLBD, and 18 μM TlpBLBD with 200 μM sodium decanoate, leucine, proline, phenylalanine, pentadecanoic acid, and arginine (as a negative control). Upper panels contain the raw titration data and the lower panels show the integrated and dilution-corrected peak areas of the raw data. Data were fitted with the 'one binding site model' of the MicroCal version of ORIGIN (Amherst, MA). Abbreviations: Asn (asparagine), Gln (glutamine), Gly (glycine), Sali (salicylic acid), Trp (tryptophan), DeNa (sodium decanoate), Leu (leucine), Ala (alanine), Val (valine), Cys (cysteine), Met (methionine), Thr (threonine), Ser (serine), Pro (proline), His (histidine), Gluc (gluconic acid), DTT (dl-dithiothreitol), Phe (phenylalanine), Malt (maltose), Fruc (fructose), Inos (inosine), PeDe (pentadecanoic acid), and Dulc (dulcitol).

Figure 4 The chemotaxis index of the different *mcp* gene complementary strains to arginine and microcalorimetric titration of McpRLBD with arginine. (A) The chemotaxis index of the different *mcp* gene complementary strains to arginine. The black dotted line represents a chemotaxis index of 0.5. The concentration of arginine was 1 mM. Data for each strain are the means of thirteen biological replicates. Error bars represent the standard error of thirteen

biological replicates. Different letters above the bars indicate significant differences ($P \leq 0.05$). (B) Titration of 15 μM McpRLBD with 500 μM arginine, and alanine (as a negative control). Upper panels contain the titration raw data and the lower panels show the integrated and dilution-corrected peak areas of the raw data. Data were fitted with the 'one binding site model' of the MicroCal version of ORIGIN (Amherst, MA).

Figure 5 Chemotactic responses of SQR9Δ*8mcp* complemented the wild type or mutated *mcpR* to arginine. The concentration of arginine was 1 mM. Data for each strain are the means of thirteen biological replicates. Error bars represent the standard error of thirteen biological replicates. Different letters above the bars indicate significant differences ($P \leq 0.05$).

Figure 6 Proposed model of the chemotaxis mobility of *B. amyloliquefaciens* SQR9 towards cucumber root-secreted compounds mediated by different chemoreceptors.

679

680 **Table 1.** Bacterial strains and plasmids used in this study.

Strains or plasmid	Characteristics	Source or reference
Plasmids		
pTPC	pMD19-T harboring the PC cassette	(Zhou et al., 2017)
pNW33N	Cm^R, *E. coli-Bacillus* shuttle vector	(Zhou et al., 2017)
p7S6	Spc^R, pMD18-T ligated with *spc* gene	(Yan et al., 2008)
pET-28a	Expression vector	Novagen
pET-28a-McpALBD	pET28a derivative for expression of McpALBD	This work
pET-28a-McpBLBD	pET28a derivative for expression of McpBLBD	This work
pET-28a-McpCLBD	pET28a derivative for expression of McpCLBD	This work
pET-28a-TlpALBD	pET28a derivative for expression of TlpALBD	This work
pET-28a-TlpBLBD	pET28a derivative for expression of TlpBLBD	This work
pET-28a-McpRLBD	pET28a derivative for expression of McpRLBD	This work
Strains		
B. amyloliquefaciens		
SQR9	Wild-type isolate	(Cao et al., 2011)
SQR9Δ*8mcp*	Deletion in all eight putative *mcp* genes	This work
SQR9Δ*8mcp*/*mcpA*	Cm^R, SQR9Δ*8mcp* with *mcpA* gene	This work
SQR9Δ*8mcp*/*mcpB*	Cm^R, SQR9Δ*8mcp* with *mcpB* gene	This work
SQR9Δ*8mcp*/*mcpC*	Spc^R, SQR9Δ*8mcp* with *mcpC* gene	This work
SQR9Δ*8mcp*/*tlpA*	Cm^R, SQR9Δ*8mcp* with *tlpA* gene	This work
SQR9Δ*8mcp*/*tlpB*	Cm^R, SQR9Δ*8mcp* with *tlpB* gene	This work
SQR9Δ*8mcp*/*mcpR*	Spc^R, SQR9Δ*8mcp* with *mcpR* gene	This work
SQR9Δ*8mcp*/*hemAT*	Cm^R, SQR9Δ*8mcp* with *hemAT* gene	This work
SQR9Δ*8mcp*/*yfmS*	Cm^R, SQR9Δ*8mcp* with *yfmS* gene	This work
E. coli		
BL21 (DE3)	F^- *ompT hsdSB*(rB^-mB^-) *gal dcm* λDE3 (harboring gene 1 of the RNA polymerase from the phage T7 under the *PlacUV5* promoter)	Invitrogen (Shanghai, China)
Top 10	F^- *mcrA* Δ*(mrr-hsdRMS-mcrBC)* ψ80 *lacZ* ΔM15 Δ*lacX74 nupG recA1 araD139*Δ*(ara-leu) 7697 galE15 galK 16 rpsL* (Str^R) *end A1*λ^-	Invitrogen (Shanghai, China)

681 Cm^R chloramphenicol resistance, Spc^R spectinomycin resistance

682 **Table 2.** Ranking and summary of the chemotaxis index (I_{30}) of SQR9 in response to the 98

683 targeted compounds.

Substances [a]		SQR9		SQR9Δ*8mcp*	
Ranking	**Numbers**	I_{30} [bc]	**Standard Error** [c]	I_{30} [bc]	**Standard Error** [c]
0.8~1.0	**23**				
Valine [d]		0.99	0.0026	0.48	0.052
Glutamine		0.99	0.0017	0.51	0.047
Serine		0.99	0.0018	0.53	0.049
Threonine		0.98	0.0024	0.49	0.036
Succinic acid		0.98	0.0030	0.43	0.049
Cystine		0.98	0.0034	0.47	0.029
DL-Malic acid		0.98	0.0038	0.53	0.057
Gluconic acid		0.97	0.0035	0.49	0.039
Asparagine		0.97	0.0071	0.47	0.039
Citric acid		0.95	0.016	0.47	0.019
D-Maltose		0.94	0.0048	0.54	0.030
Methionine		0.93	0.016	0.47	0.032
Alanine		0.93	0.014	0.55	0.040
Leucine		0.93	0.036	0.45	0.043
Arginine		0.91	0.027	0.55	0.029
Histidine		0.90	0.022	0.47	0.064
Isoleucine		0.90	0.0089	0.53	0.029
Glycine		0.88	0.031	0.58	0.061
Fumaric acid		0.86	0.019	0.57	0.027
Proline		0.81	0.035	0.57	0.062
Dulcitol		0.81	0.028	0.48	0.075
Lysine		0.81	0.015	0.51	0.038
D-Mannose		0.81	0.026	0.50	0.062
0.6~0.8	**16**				
Adipic acid		0.79	0.022	0.52	0.026
Glutamic acid		0.78	0.019	0.52	0.046
Phthalic acid		0.77	0.019	0.48	0.033
Aspartic acid		0.76	0.078	0.51	0.058
Fructose		0.74	0.033	0.52	0.039
Tryptophan		0.73	0.025	0.50	0.021
Phenylalanine		0.73	0.038	0.50	0.029
DL-Glyceric acid		0.72	0.025	0.50	0.037
Dehydroascorbic acid		0.71	0.048	0.50	0.037
Oxalic acid		0.70	0.030	0.45	0.054

Ribitol	0.69	0.038	0.50	0.055
Tyrosine	0.67	0.025	0.49	0.023
D(+)-Ribose	0.63	0.033	0.45	0.028
Inosine	0.63	0.050	0.50	0.058
3-Hydroxypropionic acid	0.62	0.042	0.49	0.038
D-(+)-Fucose	0.61	0.029	0.48	0.049
0.4~0.6 54	**Please see Table S1**			
0.0~0.4 5				
DL-Dithiothreitol	0.31	0.080	0.49	0.041
Salicylic acid	0.29	0.023	0.51	0.034
Hydroxycarbamate	0.29	0.041	0.51	0.045
Pentadecanoic acid	0.20	0.016	0.49	0.043
Sodium decanoate	0.16	0.028	0.50	0.061

Note: [a] Compounds were used at a concentration of 1 mM. [b] When the I_{30} was between 0.4 and 0.6, this was considered to be no chemotaxis response. When the I_{30} was less than 0.4, the compound was considered to be repellent. When the I_{30} was more than 0.6, the compound was considered to be an attractant. [c] Data for each compound are the means for the thirteen biological replicates. Error bars represent the standard error from the mean. [d] All the 20 amino acids are L-amino acids.

Table 3. Summary of the corresponding ligands of the six chemoreceptors with an extracellular LBD region in *B. amyloliquefaciens* SQR9 and comparison with *B. subtilis* OI1085.

MCP	Ligands information			
	Dominant/Involved [a]	**Category**	**Compounds**	**In *B. subtilis*** [b]
McpA	Dominant	Amino acids	aspartic acid *, glutamic acid *, isoleucine *, lysine *, tyrosine *	glucose (r) [c], α-methylglucoside (r)
		Acids	phthalic acid *, citric acid *, oxalic acid *, malic acid, succinic acid, fumaric acid, adipic acid, dehydroascorbic acid *, glyceric acid, 3-hydroxypropionic acid	
		Others	ribitol *, mannose *, ribose, fucose, hydroxycarbamate (r)	
	Involved		sodium decanoate (r), serine, gluconic acid, fructose	
McpB	Dominant	Amino acids	glycine *, tryptophan *, asparagine *, glutamine *	asparagine, aspirate, glutamine, glutamate, and histidine
		Acids	salicylic acid (r), sodium decanoate (r)	
	Involved		adipic acid, ribose, glyceric acid, 3-hydroxypropionic acid, serine, cystine, methionine, gluconic acid, fructose	
McpC	Dominant	Amino acids	valine *, alanine *, proline *, leucine *, histidine *, serine, threonine, cystine, methionine	all amino acids except asparagine, tryptophan, and histidine
		Acids	gluconic acid	
	Involved		succinic acid, maltose	
TlpA	Dominant		DL-dithiothreitol * (r)	Unknown
	Involved		hydroxycarbamate (r), sodium decanoate (r), gluconic acid, maltose	
TlpB	Dominant	Amino acids	phenylalanine *	Unknown
		Acids	pentadecanoic acid * (r)	
		Others	dulcitol *, inosine *, maltose, fructose	
	Involved		malic acid, succinic acid, fumaric acid, ribose, fucose, salicylic acid (r), sodium decanoate (r), threonine, gluconic acid	
McpR	Dominant	Amino acids	arginine *	N. D. [d]
	Involved		succinic acid, fucose	

Note: [a] "Dominant" indicates that this chemoreceptor predominantly mediates the chemotaxis of SQR9 to these compounds, while "involved" means that the MCP is partially involved in chemotaxis to these chemicals.

[b] ligands identified for those orthologous proteins in *B. subtilis* OI1085 according to the previous literature.

[c] (r) means this compound is chemorepellent

[d] this MCP is absent in *B. subtilis* OI1085.

* these compounds were only sensed by the single chemoreceptor.

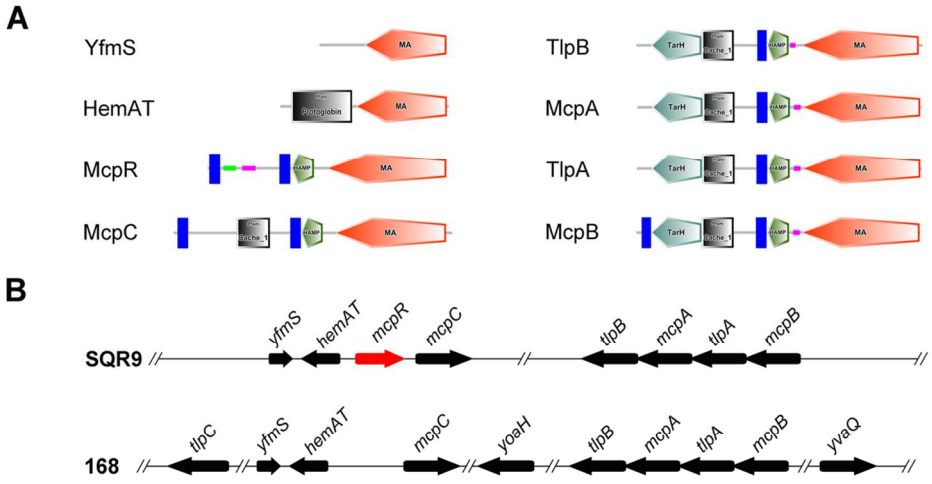

110x60mm (300 x 300 DPI)

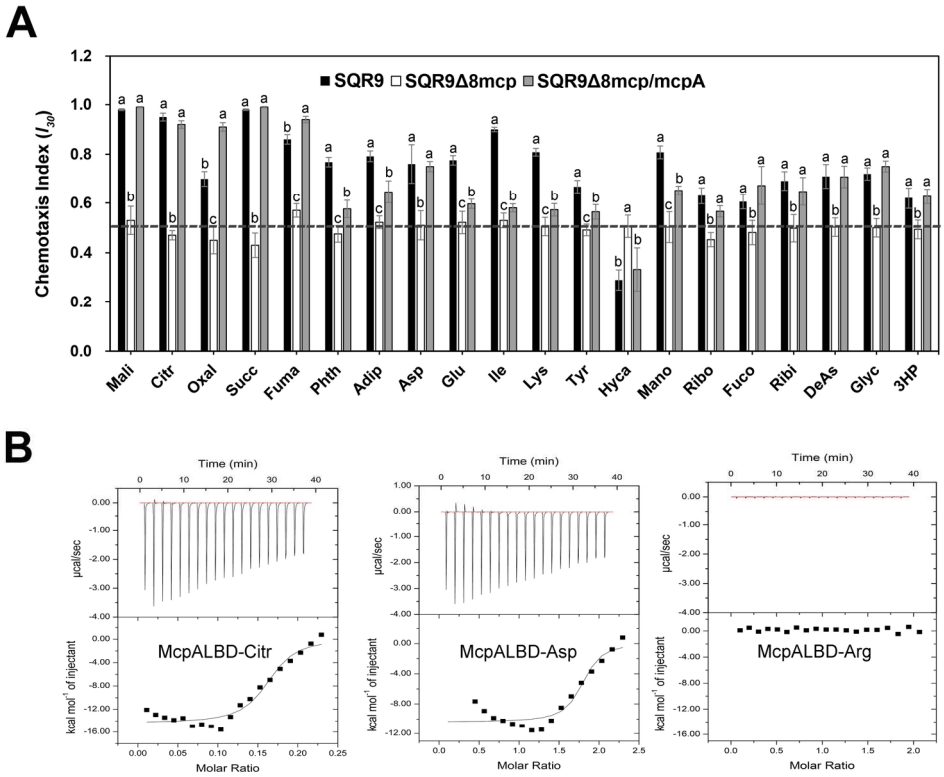

167x143mm (300 x 300 DPI)

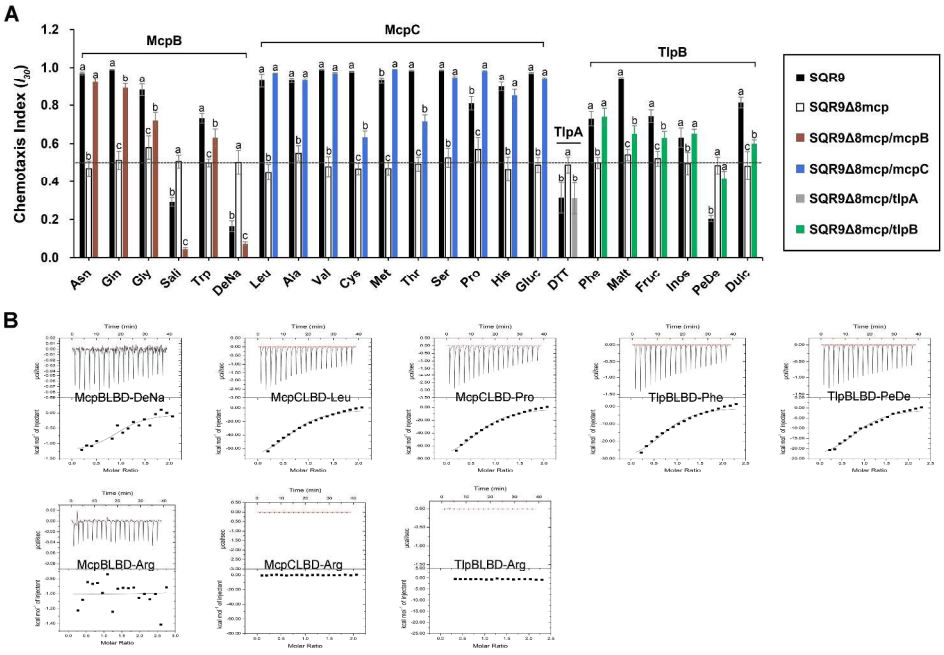

463x318mm (300 x 300 DPI)

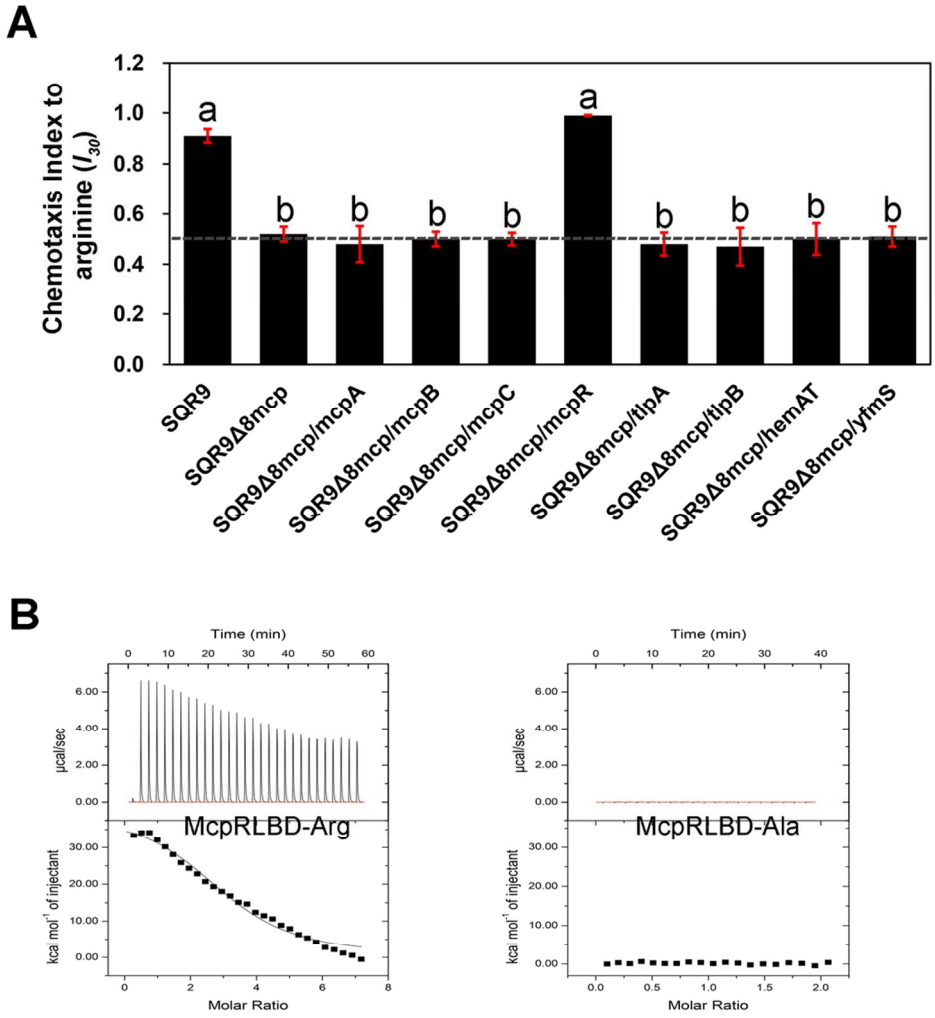

102x109mm (300 x 300 DPI)

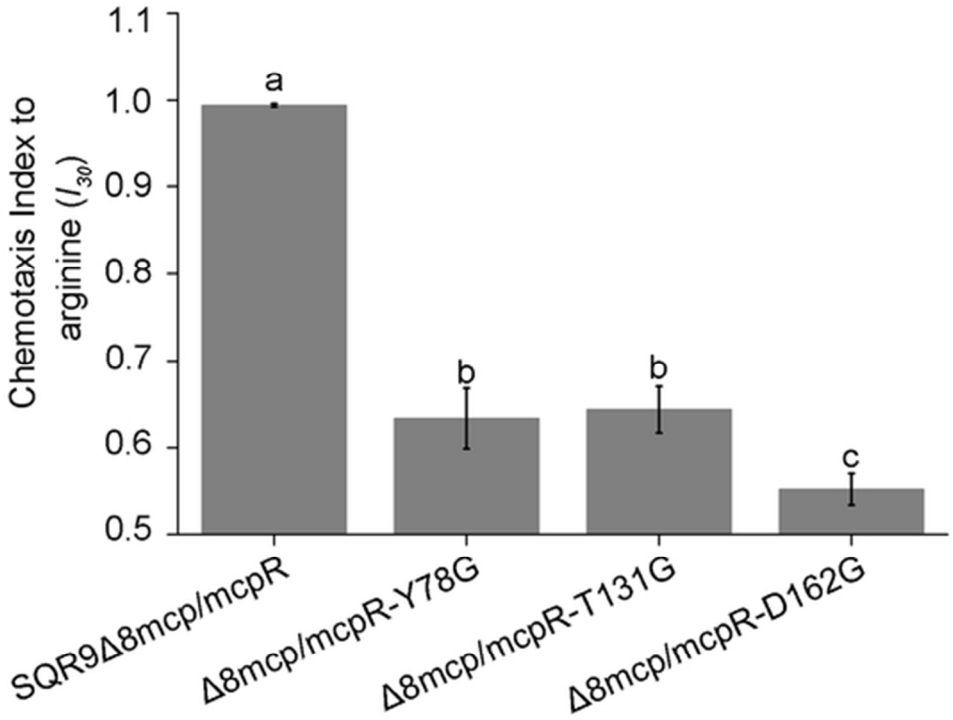

47x36mm (300 x 300 DPI)

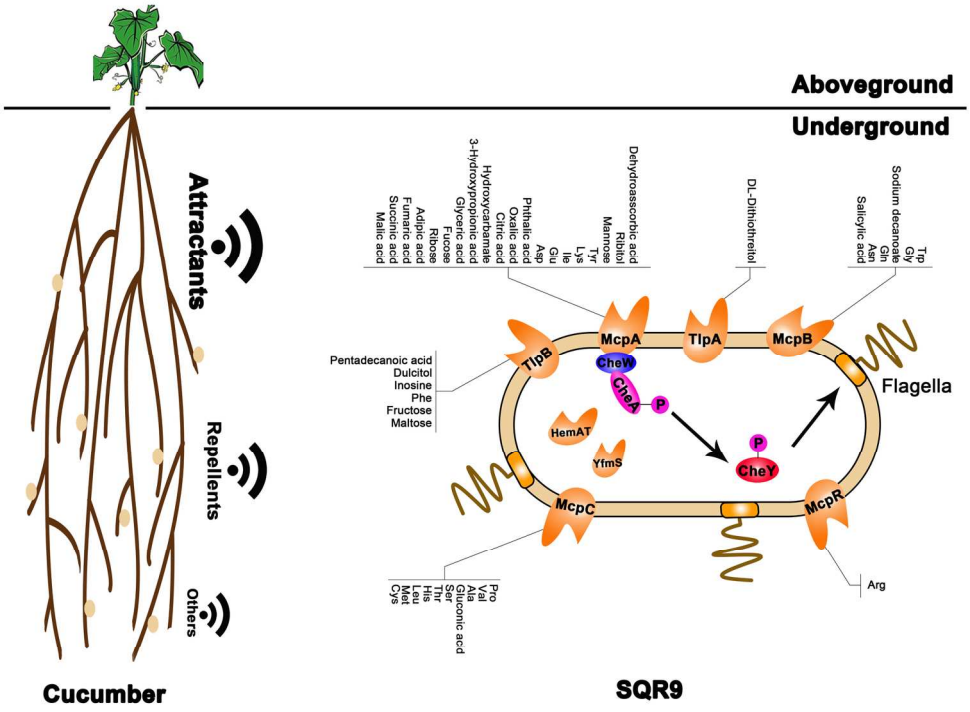

164x128mm (300 x 300 DPI)

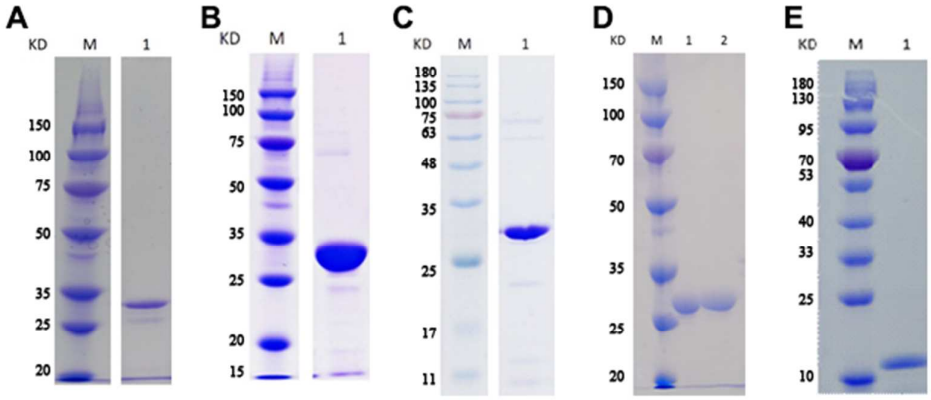

Figure S1 SDS-PAGE analysis of the proteins after purification. (A) The purified McpALBD protein. (B) The purified McpBLBD protein. (C) The purified McpCLBD protein. (D) The purified TlpALBD (left) and TlpBLBD protein (right). (E) The purified McpRLBD protein.

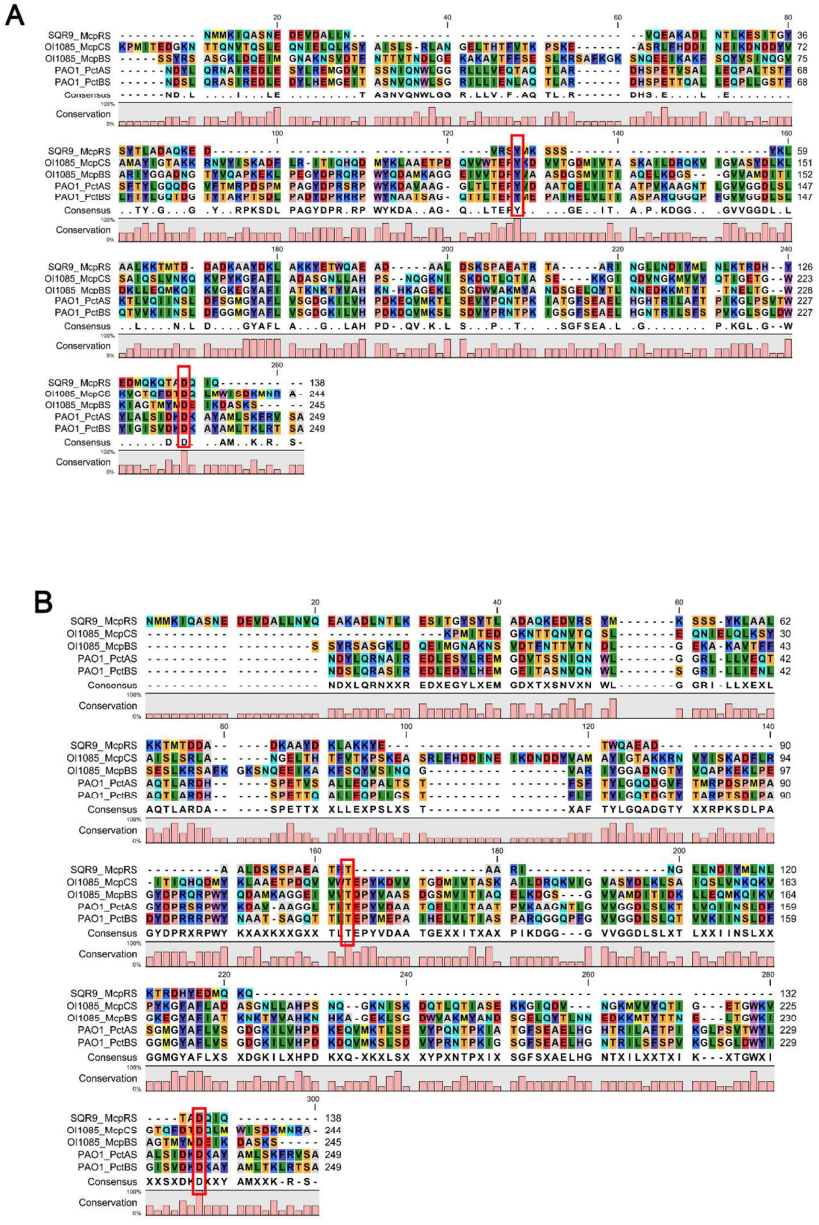

Figure S2 Sequence alignments of chemoreceptor sensing domains performed by ClustalW (A) and MAFFT (B). The aligned amino acid sequences were from selected chemoreceptors, spanning the TM1 and TM2 helices. Conserved residues are shown in *red boxes*. SQR9, *Bacillus amyloliquefaciens* SQR9; OI1085, *Bacillus subtilis* OI1085; PAO1, *Pseudomonas aeruginosa* PAO1.

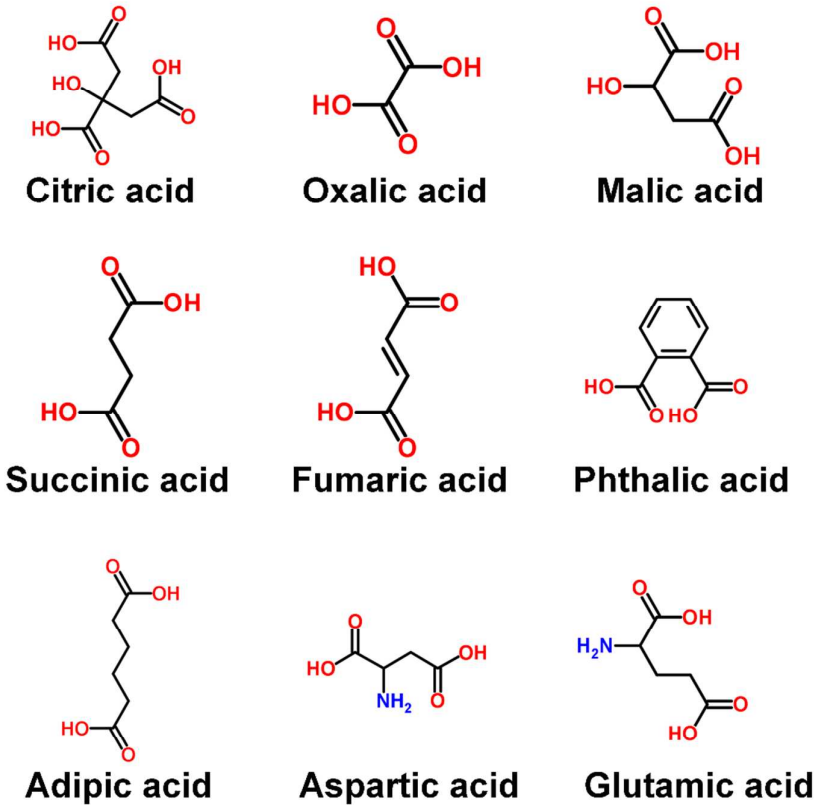

Figure S3 Nine compounds with carboxyl groups at both ends of the chains within the 44 attractants or repellents. All the nine compounds were sensed by receptor McpA in SQR9.

Table S1. The 54 chemical compounds not chemotactically responded by *B. amyloliquefaciens* SQR9.

Substances [a]	Chemotaxis Index (I_{30}) [bc]	Standard Error [c]
D-Mannitol	0.58	0.032
1-Monostearin	0.56	0.038
Glucose	0.56	0.033
Glutaric acid	0.56	0.036
DL-3-aminoisobutyric acid	0.55	0.043
Cyclohexylamine	0.55	0.062
Myo-inositol	0.55	0.047
D-Glucose-6-phosphate	0.53	0.045
D-Maltotriitol	0.53	0.040
Stigmasterol	0.53	0.023
Nicotinic acid	0.53	0.049
Hydroxylamine	0.52	0.029
p-Hydroxybenzoic acid	0.52	0.041
Sucrose	0.52	0.048
L-Threonic acid	0.52	0.023
D-Sorbitol	0.52	0.044
Raffinose	0.51	0.060
D-fructose-6-phosphate	0.51	0.058
4-hydroxybenzoate	0.51	0.037
Benzoic acid	0.51	0.035
D-xylulose	0.51	0.044
Shikimic acid	0.50	0.042
Maltitol	0.50	0.050
Guanosine	0.50	0.032
Myristic acid	0.49	0.048
N-Acetyl-D-Galactosamine	0.49	0.032
Nonivamide	0.49	0.072
D-tagatose	0.49	0.016
Palmitoleic acid	0.49	0.017
Palmitic acid	0.49	0.017
D(+)-Cellobiose	0.49	0.021
D-Xylose	0.49	0.023
Azelaic acid	0.49	0.043
1,3-Dihydroxyacetone dimer	0.49	0.021
N-Acetyl-d-mannosamine	0.49	0.044

1-Monopalmitin	0.48	0.029
Stearic acid	0.48	0.047
4-Aminobutyric acid	0.48	0.046
Galactinol	0.47	0.043
Urea	0.47	0.064
Lactose	0.47	0.052
Uracil	0.46	0.049
Nicotinamide	0.45	0.042
Beta-Glycerolphosphate	0.45	0.050
Glycolic acid	0.45	0.040
Putrescine	0.44	0.041
Biuret	0.44	0.051
Parabanic acid	0.44	0.040
Lauric acid	0.43	0.040
Tyramine	0.42	0.028
Erythritol	0.41	0.032
Vanillic acid	0.41	0.045
Xylitol	0.40	0.040
Acetophenone	0.40	0.055

Note: [a] Compounds were used at a concentration of 1mM. [b] When the I_{30} was between 0.4 and 0.6, the chemotaxis was considered as no response. [c] Data for each compound are the means for thirteen biological replicates. Error bars represent the standard error from the mean.

Table S2. The overview of *mcpR*-containing strains.

Species	*McpR*-containing strains		Total number of strains from NCBI	Percentage of *mcpR*-containing strains (%)
	Name	Total number		
Bacillus amyloliquefaciens	SQR9, Lx-11, UMAF6614, WP_072177115.1, Jxnuwx-1, EGD-AQ14, XK-4-1, RHNK22, 629, Y14, B4140, MBE1283, LPL-K103, LFB112, H57, GD4a, L-H15, LM2303, B15, Bs006, EBL11, UMAF6639, CC178, HB-26, 11B91, SRCM101294, LL3, RD7-7, K2, CMW1, DSM7	31	56	55.4
Bacillus velezensis	SSBW-19, 9912D, NAU-B3, SK19.001, 2A-2B, CAU B946, JJ-D34, SYBC H47, SRCM100731, GH1-13, AS43.3, SSBW-18, M27, CFSAN034340, AP183, B25, GR4-5, SB1216, TrigoCor1448, UCMB5036, WP_029973159.1, UCMB5113, CFSAN034338, AP194, KACC18228, K26, M75, UCMB5033, CC09, YAU B9601-Y2	30	56	53.6
Bacillus nakamurai	B-41092, NRRL B-41091	2	16	12.5
Bacillus subtilis	B-1	1	56	1.8
Bacillus sp.	Pc3, LK7, UNC69MF	3	unknown	unknown

Table S3. Chemotaxis index of the 18 compounds sensed by more than one *mcp*-gene for *B. amyloliquefaciens* SQR9, chemoreceptor-deficient mutant SQR9Δ8mcp and the single-*mcp*-gene complementary strains.

Substances [a]	**Chemotaxis Index (I_{30})** [bc]									
	SQR9	**SQR9Δ8mcp**	**SQR9Δ8mcp/mcpA**	**SQR9Δ8mcp/mcpB**	**SQR9Δ8mcp/mcpC**	**SQR9Δ8mcp/mcpR**	**SQR9Δ8mcp/tlpA**	**SQR9Δ8mcp/tlpB**	**SQR9Δ8mcp/hemAT**	**SQR9Δ8mcp/yfmS**
Amino acids										
Cysteine	0.98	0.47	0.46	0.61	0.63	0.51	0.52	0.49	0.49	0.50
Methionine	0.93	0.47	0.53	0.64	0.99	0.43	0.46	0.48	0.50	0.51
Serine	0.99	0.53	0.68	0.66	0.95	0.51	0.54	0.54	0.49	0.50
Threonine	0.98	0.49	0.51	0.52	0.72	0.51	0.48	0.66	0.49	0.53
Acids										
fumaric acid	0.86	0.57	0.94	0.58	0.51	0.53	0.51	0.69	0.49	0.54
Malic acid	0.98	0.53	0.99	0.56	0.55	0.51	0.53	0.69	0.49	0.51
Succinic acid	0.98	0.43	0.99	0.48	0.66	0.66	0.48	0.79	0.45	0.52
Adipic acid	0.79	0.52	0.65	0.23	0.44	0.46	0.46	0.52	0.53	0.50
Glyceric acid	0.72	0.50	0.75	0.34	0.51	0.50	0.49	0.50	0.49	0.52
Gluconic acid	0.97	0.49	0.66	0.11	0.94	0.51	0.68	0.61	0.51	0.52
Sodium decanoate	0.16	0.50	0.14	0.07	0.50	0.50	0.17	0.16	0.49	0.49
Salicylic acid	0.29	0.51	0.48	0.05	0.53	0.51	0.47	0.29	0.44	0.46
3-Hydroxypropionic acid	0.62	0.49	0.63	0.61	0.51	0.53	0.49	0.45	0.45	0.47

Others										
Fructose	0.74	0.52	0.62	0.62	0.56	0.53	0.51	0.63	0.49	0.52
Fucose	0.61	0.48	0.67	0.41	0.51	0.65	0.49	0.66	0.48	0.51
Maltose	0.94	0.54	0.53	0.48	0.62	0.44	0.61	0.65	0.48	0.52
Ribose	0.63	0.45	0.64	0.54	0.51	0.43	0.47	0.25	0.52	0.48
Hydroxycarbamate	0.29	0.51	0.33	0.47	0.53	0.49	0.36	0.46	0.48	0.47

Substances [a]	**Standard Error** [c]									
	SQR9	**SQR9Δ8mcp**	**SQR9Δ8mcp/mcpA**	**SQR9Δ8mcp/mcpB**	**SQR9Δ8mcp/mcpC**	**SQR9Δ8mcp/mcpR**	**SQR9Δ8mcp/tlpA**	**SQR9Δ8mcp/tlpB**	**SQR9Δ8mcp/hemAT**	**SQR9Δ8mcp/ymS**
Amino acids										
Cysteine	0.003	0.029	0.046	0.034	0.032	0.049	0.034	0.052	0.041	0.060
Methionine	0.016	0.032	0.038	0.037	0.001	0.045	0.019	0.028	0.027	0.058
Serine	0.002	0.049	0.017	0.030	0.006	0.040	0.042	0.038	0.036	0.054
Threonine	0.002	0.036	0.025	0.031	0.033	0.043	0.040	0.036	0.021	0.055
Acids										
fumaric acid	0.019	0.027	0.013	0.064	0.075	0.042	0.030	0.042	0.064	0.031
Malic acid	0.004	0.057	0.002	0.039	0.055	0.060	0.023	0.049	0.046	0.045
Succinic acid	0.003	0.049	0.002	0.068	0.072	0.049	0.044	0.023	0.040	0.021
Adipic acid	0.022	0.026	0.045	0.027	0.045	0.024	0.051	0.036	0.047	0.052
Glyceric acid	0.025	0.037	0.022	0.027	0.040	0.046	0.044	0.017	0.049	0.043
Gluconic acid	0.004	0.039	0.046	0.012	0.007	0.039	0.035	0.023	0.029	0.028
Sodium	0.028	0.061	0.025	0.010	0.045	0.060	0.019	0.011	0.071	0.051

decanoate										
Salicylic acid	0.023	0.034	0.021	0.007	0.033	0.044	0.051	0.052	0.024	0.042
3-Hydroxypropionic acid	0.042	0.038	0.030	0.017	0.036	0.035	0.016	0.042	0.027	0.054
Others										
Fructose	0.033	0.039	0.021	0.034	0.046	0.026	0.043	0.034	0.031	0.033
Fucose	0.029	0.049	0.078	0.045	0.064	0.027	0.008	0.043	0.031	0.047
Maltose	0.005	0.030	0.034	0.057	0.041	0.041	0.035	0.041	0.041	0.052
Ribose	0.033	0.028	0.023	0.017	0.054	0.017	0.046	0.024	0.023	0.048
Hydroxycarbamate	0.041	0.045	0.087	0.036	0.038	0.050	0.017	0.034	0.036	0.064

Note: [a] Compounds were used at a concentration of 1mM. [b] When the I_{30} was between 0.4 and 0.6, the chemotaxis was considered as no response. When the I_{30} was less than 0.4, the compound was considered as repellent. And the I_{30} was more than 0.6, the compound was considered as attractant. [c] Data for each compound are the means for thirteen biological replicates. Error bars represent the standard error from the mean

Table S4. Chemotaxis index of the 44 compounds for *hemAT* and *yfmS* gene complementary strains *B. amyloliquefaciens* SQR9Δ8mcp/hemAT and SQR9Δ8mcp/yfmS.

Substances [a]	SQR9 Δ 8mcp/hemAT		SQR9 Δ 8mcp/yfmS	
	I_{30} [bc]	Standard Error [c]	I_{30} [bc]	Standard Error [c]
Malic acid	0.49	0.046	0.51	0.045
Citric acid	0.49	0.065	0.50	0.056
Oxalic acid	0.52	0.038	0.44	0.074
Succinic acid	0.45	0.040	0.52	0.021
Fumaric acid	0.49	0.064	0.54	0.031
Salicylic acid	0.44	0.024	0.46	0.042
Phthalic acid	0.47	0.025	0.51	0.031
Adipic acid	0.53	0.047	0.50	0.052
3-Hydroxypropionic acid	0.45	0.027	0.47	0.054
Pentadecanoic acid	0.50	0.045	0.51	0.078
Dehydroasscorbic acid	0.50	0.049	0.49	0.055
Sodium decanoate	0.49	0.071	0.49	0.051
Glyceric acid	0.49	0.049	0.52	0.043
Gluconic acid	0.51	0.029	0.52	0.028
Asparagine [d]	0.41	0.045	0.47	0.030
Arginine	0.50	0.063	0.51	0.040
Isoleucine	0.51	0.021	0.50	0.037
Phenylalanine	0.49	0.064	0.50	0.075
Aspartic acid	0.46	0.036	0.51	0.069
Leucine	0.51	0.025	0.53	0.072
Glycine	0.47	0.027	0.53	0.067
Proline	0.50	0.020	0.42	0.041
Alanine	0.46	0.029	0.58	0.041
Threonine	0.49	0.021	0.53	0.055
Cysteine	0.49	0.041	0.50	0.060
Histidine	0.52	0.026	0.48	0.025
Glutamic acid	0.49	0.050	0.48	0.040
Lysine	0.53	0.026	0.52	0.042
Serine	0.49	0.036	0.50	0.054
Valine	0.51	0.031	0.51	0.054
Glutamine	0.49	0.059	0.51	0.050

Tyrosine	0.48	0.038	0.50	0.042
Tryptophan	0.52	0.017	0.49	0.070
Methionine	0.50	0.027	0.51	0.058
Fucose	0.48	0.031	0.51	0.047
Maltose	0.48	0.041	0.52	0.052
Mannose	0.49	0.034	0.51	0.048
Ribose	0.52	0.023	0.48	0.048
Fructose	0.49	0.031	0.52	0.033
Dithiothreitol	0.50	0.039	0.49	0.045
Ribitol	0.49	0.059	0.50	0.048
Dulcitol	0.48	0.048	0.49	0.023
Inosine	0.49	0.049	0.47	0.041
Hydroxycarbamate	0.48	0.036	0.47	0.064

Note: [a] Compounds were used at a concentration of 1mM. [b] When the I_{30} was between 0.4 and 0.6, the chemotaxis was considered as no response. When the I_{30} was less than 0.4, the compound was considered as repellent. And the I_{30} was more than 0.6, the compound was considered as attractant. [c] Data for each compound are the means for thirteen biological replicates. Error bars represent the standard error from the mean. [d] All the 20 amino acids are L-amino acids.

Table S5. The Chemotaxis index of 20 essential amino acids for *B. amyloliquefaciens* SQR9, chemoreceptor-deficient mutant SQR9Δ8mcp and the mcpR complementary strain SQR9Δ8mcp/mcpR.

Substances [a]	Chemotaxis Index (I_{30}) [bc]			Standard Error [c]		
	SQR9	SQR9Δ8mcp	SQR9Δ8mcp/mcpR	SQR9	SQR9Δ8mcp	SQR9Δ8mcp/mcpR
L-Valine	0.99	0.48	0.50	0.0026	0.052	0.0030
L-Glutamine	0.99	0.51	0.50	0.0017	0.047	0.075
L-Serine	0.99	0.53	0.51	0.0018	0.049	0.040
L-Threonine	0.98	0.49	0.51	0.0024	0.036	0.043
L-Cysteine	0.98	0.47	0.51	0.0035	0.029	0.049
L-Asparagine	0.97	0.47	0.47	0.0071	0.039	0.033
L-Methionine	0.93	0.47	0.43	0.016	0.032	0.045
L-Alanine	0.93	0.55	0.44	0.014	0.040	0.052
L-Leucine	0.93	0.45	0.54	0.036	0.043	0.039
L-Arginine	0.91	0.55	0.99	0.027	0.029	0.0019
L-Histidine	0.90	0.47	0.5	0.022	0.064	0.049
L-Isoleucine	0.90	0.53	0.41	0.0089	0.029	0.035
Glycine	0.88	0.58	0.46	0.031	0.061	0.046
L-Proline	0.81	0.57	0.41	0.035	0.062	0.052
L-Lysine	0.81	0.51	0.46	0.015	0.038	0.052
L-Glutamic acid	0.78	0.52	0.51	0.019	0.046	0.046
L-Aspartic acid	0.76	0.51	0.39	0.078	0.058	0.032
L-Tryptophan	0.73	0.5	0.47	0.025	0.021	0.032
L-Phenylalanine	0.73	0.5	0.5	0.038	0.029	0.021
L-Tyrosine	0.67	0.49	0.49	0.025	0.023	0.072

Note: [a] Compounds were used at a concentration of 1mM. [b] When the I_{30} was between 0.4 and 0.6, the chemotaxis was considered as no response. When the I_{30} was less than 0.4, the compound was considered as repellent. And the I_{30} was more than 0.6, the compound was considered as attractant. [c] Data for each compound are the means for thirteen biological replicates. Error bars represent the standard error from the mean.

Table S6. Primers used in this study.

Primers	Oligonucleotide sequences	Function
Δ4mcp-UF	TCTGAAACCGTCGATGTACTACGA	Delete the 4 adjacent *mcp* genes
Δ4mcp-UR	CTTGAGGGAGCAGCTTAATATGAAACGAGCTGTTTCTTTTCCTTATCTG	
Δ4mcp-BF	CAGATAAGGAAAAGAAACAGCTCGTTTCATATTAAGCTGCTCCCTCAAG	Delete the 4 adjacent *mcp* genes
Δ4mcp-BR	CGCAGTTTAAACAGGCGTAATAAATTCTGTACTTCAGCTCCAAGGCT	
Δ4mcp-PSF	AGCCTTGGAGCTGAAGTACAGAATTTATTACGCCTGTTTAAACTGCG	Delete the 4 adjacent *mcp* genes
Δ4mcp-PSR	AGTCTGAAGACGAAGAACAGCTGTAGCCGTTCGTATAATGTATGCTATACG	
Δ4mcp-DF	CGTATAGCATACATTATACGAACGGCTACAGCTGTTCTTCGTCTTCAGACT	Delete the 4 adjacent *mcp* genes
Δ4mcp-DR	GGAAGAAAGTGCTGATCACCTTTC	
Δ4mcp-VF	TGGAGGAAGCGAGAAA	Delete the 4 adjacent *mcp* genes
Δ4mcp-VR	CGAATTGTACGGGAGA	
Δ5mcp-UF	GATGGGGTCAAAGCCTTACA	Delete the *mcpC* genes
Δ5mcp-UR	GGCTGATAGAGACCGCGTTAAACCATCCCCTCCTGAGAGT	
Δ5mcp-BF	ACTCTCAGGAGGGGATGGTTTAACGCGGTCTCTATCAGCC	Delete the *mcpC* genes
Δ5mcp-BR	CGCAGTTTAAACAGGCGTAATAACCAAGGCGTGAATGGACTT	
Δ5mcp-PSF	AAGTCCATTCACGCCTTGGTTATTACGCCTGTTTAAACTGCG	Delete the *mcpC* genes
Δ5mcp-PSR	GTACGCAAGCGCGACATATTCCGTTCGTATAATGTATGCTATACG	
Δ5mcp-DF	CGTATAGCATACATTATACGAACGGAATATGTCGCGCTTGCGTAC	Delete the *mcpC* genes
Δ5mcp-DR	GGCGACTTCCTCTATCGCTT	
Δ5mcp-VF	TCGAATACCCGTTAGGA	Delete the *mcpC* genes
Δ5mcp-VR	CGATGCCCATGTCTTTA	
Δ6mcp-UF	CGGCGACCAATCATTTAATG	Delete the *mcpR* genes

Δ6mcp-UR	GGGGCAAAAGCCCGTTATTCAGATCGCCTCCTTTTTC	
Δ6mcp-BF	GAAAAAGGAGGCGATCTGAATAACGGGCTTTTGCCCC	Delete the *mcpR* genes
Δ6mcp-BR	CGCAGTTTAAACAGGCGTAATAAGCTTCCGCAAGCCGTTT	
Δ6mcp-PSF	AAACGGCTTGCGGAAGCTTATTACGCCTGTTTAAACTGCG	Delete the *mcpR* genes
Δ6mcp-PSR	GCCTTGTCCGTAATGTCACCCGTTCGTATAATGTATGCTATACG	
Δ6mcp-DF	CGTATAGCATACATTATACGAACGGGTGACATTACGGACAAGGC	Delete the *mcpR* genes
Δ6mcp-DR	TTCAATGAATTGCACCGC	
Δ6mcp-VF	TCACCCTGCCGAACATA	Delete the *mcpR* genes
Δ6mcp-VR	CCTTCTGCCTTTCCAAT	
Δ7mcp-UF	CTTTCCTGAAAGGCTGCCAA	Delete the *hemAT* genes
Δ7mcp-UR	AATATCTGGGGGAACTTATATAAAGATAAACCGACCGGCC	
Δ7mcp-BF	GGCCGGTCGGTTTATCTTTATATAAGTTCCCCCAGATATT	Delete the *hemAT* genes
Δ7mcp-BR	CGCAGTTTAAACAGGCGTAATAAAACTGATTTCTTATAATGCC	
Δ7mcp-PSF	GGCATTATAAGAAATCAGTTTTATTACGCCTGTTTAAACTGCG	Delete the *hemAT* genes
Δ7mcp-PSR	ATCTCCTGTCACTCAACGCCCGTTCGTATAATGTATGCTATACG	
Δ7mcp-DF	CGTATAGCATACATTATACGAACGGGCGTTGAGTGACAGGAGAT	Delete the *hemAT* genes
Δ7mcp-DR	AATGGTCAGGCTTGGAAAC	
Δ7mcp-VF	CGAGGTGAATCCGATAT	Delete the *hemAT* genes
Δ7mcp-VR	TGTCTGCTCTTCCCACT	
Δ8mcp-UF	ATTATCTCATTTACAGGCTC	Delete the *yfmS* genes
Δ8mcp-UR	CCGTAAGCTCCCTTTTTTTATTCTTTCACTCCTTCTTAAT	
Δ8mcp-BF	ATTAAGAAGGAGTGAAAGAATAAAAAAAGGGAGCTTACGG	Delete the *yfmS* genes
Δ8mcp-BR	CGCAGTTTAAACAGGCGTAATAAACGCTTCATCGCTTAAATCT	
Δ8mcp-PSF	AGATTTAAGCGATGAAGCGTTTATTACGCCTGTTTAAACTGCG	Delete the *yfmS* genes
Δ8mcp-PSR	TGTCATCTTGGATCAGGCTCCGTTCGTATAATGTATGCTATACG	
Δ8mcp-DF	CGTATAGCATACATTATACGAACGGAGCCTGATCCAAGATGACA	Delete the *yfmS* genes

Δ8mcp-DR	CTGGGCGCTTCCCGAAAT	
Δ8mcp-VF	ATTCTCCCGTCCACGATT	Delete the *yfmS* genes
Δ8mcp-VR	ACAAAGCCGCCTCCTATC	
amyE-UF	GAGAAGGCGTCGTAAAC	Complementation of the single gene
amyE-UR	TAACGGCAGTAAAGAGGT	
amyE-DF	TGATTATGTGCAGAATGGT	Complementation of the single gene
amyE-DR	TCTCGATAATATGGTAGGC	
mcpA-CmF	ATTCAAAACCTCTTTACTGCCGTTAGCATAAAGTGTAAAGCCTGGGG	Complementation of the *mcpA* gene
mcpA-CmR	TATGACGAAACGATTTAAAATAGATAATGTGGAATTGGGAACGGAAA	
mcpA-F	ATCTATTTTAAATCGTTT	Complementation of the *mcpA* gene
mcpA-R	ATACAAACCATTCTGCACATAATCACTGCGCGCCCCCTATCTT	
mcpA-PF	TTAGTCTTTTAGACTTAATTAATTAAGCTGCTCCCTCAAGTGTGATAC	Complementation of the *mcpA* gene
mcpA-PR	ATACAAACCATTCTGCACATAATCACTGCGCGCCCCCTATCTT	
mcpB-CmF	ATTCAAAACCTCTTTACTGCCGTTAGCATAAAGTGTAAAGCCTGGGG	Complementation of the *mcpB* gene
mcpB-CmR	ATTAACGAAACAATTTAAAATCAACAATGTGGAATTGGGAACGGAAA	
mcpB-F	GTTGATTTTAAATTGTTT	Complementation of the *mcpB* gene
mcpB-R	ATACAAACCATTCTGCACATAATCACTGCGCGCCCCCTATCTT	
mcpC-F	ACCTCTTTACTGCCGTTATAAGGCGGAGCTGTCGGC	Complementation of the *mcpC* gene
mcpC-R	CGTTACGTTATTAGTTATTGCGCTTTCCTCCCCTGA	
mcpC-SpcF	TCAGGGGAGGAAAGCGCAATAACTAATAACGTAACG	Complementation of the *mcpC* gene
mcpC-SpcR	ACCATTCTGCACATAATCACGTATAATGTATGCTATA	
tlpA-CmF	ATTCAAAACCTCTTTACTGCCGTTAGCATAAAGTGTAAAGCCTGGGG	Complementation of the *tlpA* gene
tlpA-CmR	GACAAAGCGTTTTAAGATAAACTCTAATGTGGAATTGGGAACGGAAA	
tlpA-F	AGAGTTTATCTTAAAACG	Complementation of the *tlpA* gene
tlpA-R	ATACAAACCATTCTGCACATAATCACTGCGCGCCCCCTATCTT	
tlpA-PF	GCGTCCTTTTTTACTAATTAAGCTGCTCCCTCAAGTGTGATA	Complementation of the *tlpA* gene

tlpA-PR	ATACAAACCATTCTGCACATAATCACTGCGCGCCCCCTATCTT	
tlpB-CmF	ATTCAAAACCTCTTTACTGCCGTTAGCATAAAGTGTAAAGCCTGGGG	Complementation of the *tlpB* gene
tlpB-CmR	TCAGTCTGAAGACGAAGAACAGCTGAATGTGGAATTGGGAACGGAAA	
tlpB-F	CAGCTGTTCTTCGTCTTC	Complementation of the *tlpB* gene
tlpB-R	ATACAAACCATTCTGCACATAATCACTGCGCGCCCCCTATCTT	
tlpB-PF	GGGTGTTCTATGACCTATTAATTAAGCTGCTCCCTCAAGTGTGAT	Complementation of the *tlpB* gene
tlpB-PR	ATACAAACCATTCTGCACATAATCACTGCGCGCCCCCTATCTT	
mcpR-PF	TTTCCGTTCCCAATTCCACATTTAAATTTTCTGCAAAAAC	Complementation of the *mcpR* gene
mcpR-PR	CAGCCTTGTCCGTAATGTCACTGAAACTCTCCTTTTGTT	
mcpR-F	GAAAAAAACAAAAGGAGAGTTTCAGTGACATTACGGACAAGG	Complementation of the *mcpR* gene
mcpR-R	CGTTACGTTATTAGTTATCAAAGTAAACCGGCGGA	
mcpR-SpcF	TCCGCCGGTTTACTTTGATAACTAATAACGTAACG	Complementation of the *mcpR* gene
mcpR-SpcR	ACCATTCTGCACATAATCACGTATAATGTATGCTATA	
hemAT-CmF	ATTCAAAACCTCTTTACTGCCGTTAGCATAAAGTGTAAAGCCTGGGG	Complementation of the *hemAT* gene
hemAT-CmR	ATTCACTTGTTATCCTTACAGAAGAATAAAATGTGGAATTGGGAACGGAAA	
hemAT-F	TTATTCTTCTGTAAGGATAACAAG	Complementation of the *hemAT* gene
hemAT-R	ATACAAACCATTCTGCACATAATCAGATTTCTTATAATGCCGACG	
yfmS-CmF	ATTCAAAACCTCTTTACTGCCGTTAGCATAAAGTGTAAAGCCTGGGG	Complementation of the *yfmS* gene
yfmS-CmR	GAATTTTCAGGAGGACCCATAATGTGGAATTGGGAACGGAAA	
yfmS-PF	TTTCCGTTCCCAATTCCACATTATGGGTCCTCCTGAAAATTC	Complementation of the *yfmS* gene
yfmS-PR	TCTTTCACTCCTTCTTAGTAAACATCTCCCTTTCACC	
yfmS-F	GGTGAAAGGGAGATGTTTACTAAGAAGGAGTGAAAGA	Complementation of the *yfmS* gene
yfmS-R	ATACAAACCATTCTGCACATAATCATTATGACTCTCCGAGTA	
pET28a-McpALBD-F	GGAATTCCATATGGCTTTTATCGCCTATCAA	Expression of the LBD of McpA
pET28a-McpALBD-R	CCCAAGCTTTTACGGCAGGGCCGCTTC	
pET28a-McpBLBD-F	GGAATTCCATATGGAATTCAGTTCATACCAT	Expression of the LBD of McpB

pET28a-McpBLBD-R	CCCAAGCTTCTACGGTTGTGAGGCGTC	
pET28a-McpCLBD-F	GGAATTCCATATGAAGCCGATGATGACGGAG	Expression of the LBD of McpC
pET28a-McpCLBD-R	CCCAAGCTTTTACATTTTGTCGGCTAC	
pET28a-TlpALBD-F	GGAATTCCATATGGCTGCCGGCGCCTACCGT	Expression of the LBD of TlpA
pET28a-TlpALBD-R	CCCAAGCTTTTACGGTCTTGCCGCATC	
pET28a-TlpBLBD-F	GGAATTCCATATGGCCTACTTCAGCTACCAA	Expression of the LBD of TlpB
pET28a-TlpBLBD-R	CCCAAGCTTCTACATTTTCATGACAGG	
pET28a-McpRLBD-F	GGAATTCCATATGTCAAATGAAGATGAAGTG	Expression of the LBD of McpR
pET28a-McpRLBD-R	CCCAAGCTTTTACTGAATCTGGTCAGC	